6-2018

Petrology and thermodynamic modeling of amphibolite facies rocks of the Blåhø Nappe of the Middle Allochthon, Scandinavian Caledonides in Norway

Maria Van Nostrand

Petrology and thermodynamic modeling of amphibolite facies rocks of the Blåhø Nappe of the Middle Allochthon, Scandinavian Caledonides in Norway

by:

Maria Van Nostrand

Advisor:

Professor Kurt Hollocher

****

Submitted in partial fulfillment of the requirements

for Honors in the Department of Geology

UNION COLLEGE

June, 2018

ABSTRACT

The Scandinavian Caledonides are an orogenic belt formed when Baltica collided with Laurentia during the late Silurian to early Devonian (Scandian, ~426–390 Ma, Gee et al., 2008). The thrust sheets forming the belt are divided into the Lower, Middle, Upper, and Uppermost Allochthons derived, respectively, from the Baltican margin and regions progressively farther outboard. This study focuses on the Blåhø Nappe, part of the Middle Allochthon, which is generally presumed to have been from an Early Paleozoic volcanic arc off the Baltican margin. The Blåhø Nappe contains abundant igneous and sedimentary rocks, metamorphosed almost entirely at amphibolite facies, but contains scattered eclogites that indicate prior metamorphism at high pressure. The host amphibolites adjacent to eclogites retain microstructures indicating that the amphibolites originated from retrograded eclogites, and thus were once eclogites themselves. Rocks away from the eclogites, however, have no textural evidence of having been eclogites, and presumably have been retrograded from eclogite and thoroughly recrystallized.

Using textural evidence, mineral analyses, and thermodynamic modeling, we studied the conditions under which the host amphibolites transformed from eclogites during tectonic escape from great depth. 41 rock samples, mostly amphibolites from different sites in the Blåhø Nappe, were made into polished thin sections, with mineral assemblages and textures observed with a polarized light microscope. BSE imaging and quantitative analyses (standards-based EDS) were done on selected samples, targeting particular textures and low-variance assemblages. Analyses were modified to fit thermodynamic solution model stoichiometric constraints, and combined as system compositions for thermodynamic modeling with Perple_X. The modal and mineral

compositional results were compared across the model T-P space to the mineral modes and compositions given to the model. Where the modal and compositional criteria matched (within uncertainties) was presumed to be the best estimate of the T-P conditions of last equilibration of that assemblage. Multiple samples giving best results at the same T-P conditions gave confidence that those T-P estimates were geologically meaningful.

Textural evidence (such as garnet-rimming symplectites and pyroxenes rich in plagioclase inclusions and exsolution lamellae) strongly indicates that the amphibolites were once eclogites themselves. Other workers show that the eclogites formed in T-P conditions of ~550 - 750°C 15 – 35 kbars. Remnant eclogite retrograde textures in Blåhø Nappe samples apparently record intermediate conditions of ~550 - 800 °C, 7 - 10 kbars. as eclogites recrystallized into amphibolites. Amphibolite matrix apparently deformed and partially reequilibrated at T-P conditions of ~475 - 525 °C, 5-8 kbars. These temperatures and pressures of metamorphism could only be determined by comparing nearby samples, because the complexity of the mineral textures and chemistry (e.g. zoning), made it very difficult to choose apparent equilibrium textures without the models.

ACKNOWLEDGEMENTS

I would like to thank Professor Hollocher for his guidance during this study, Peter Robinson and Professor Hollocher for sample collection, the Union College Geology Department for providing the laboratory equipment, NSF for providing funding for the SEM, the Union College Undergraduate Summer Research Program for supporting this research, and the Endowed Fund for S.T.E.M. Research for funding my eight weeks of summer research.

TABLE OF CONTENTS

LIST OF FIGURES

LIST OF TABLES

INTRODUCTION / GEOLOGIC SETTING

The Scandinavian Caledonides are a complex late Silurian to early Devonian (~426 - 390 Ma, Scandian) orogenic belt (Gee et al., 2008). This orogenic belt is the consequence of a collision between Baltica and Laurentia (specifically, Greenland), in a multi-stage closing of part of the Iapetus Ocean (Gee et al., 2008). The stacked thrust sheets that make up the Scandinavian Caledonides were transported over hundreds of kilometers onto Baltica (Gee et al., 2008), and are divided into four allochthons Lower, Middle, Upper and Uppermost Allochthons (Figure 1).

The distinction between the different allochthons based in part on their inferred pre-collision geographic affinity and displacement from their original source. The higher the

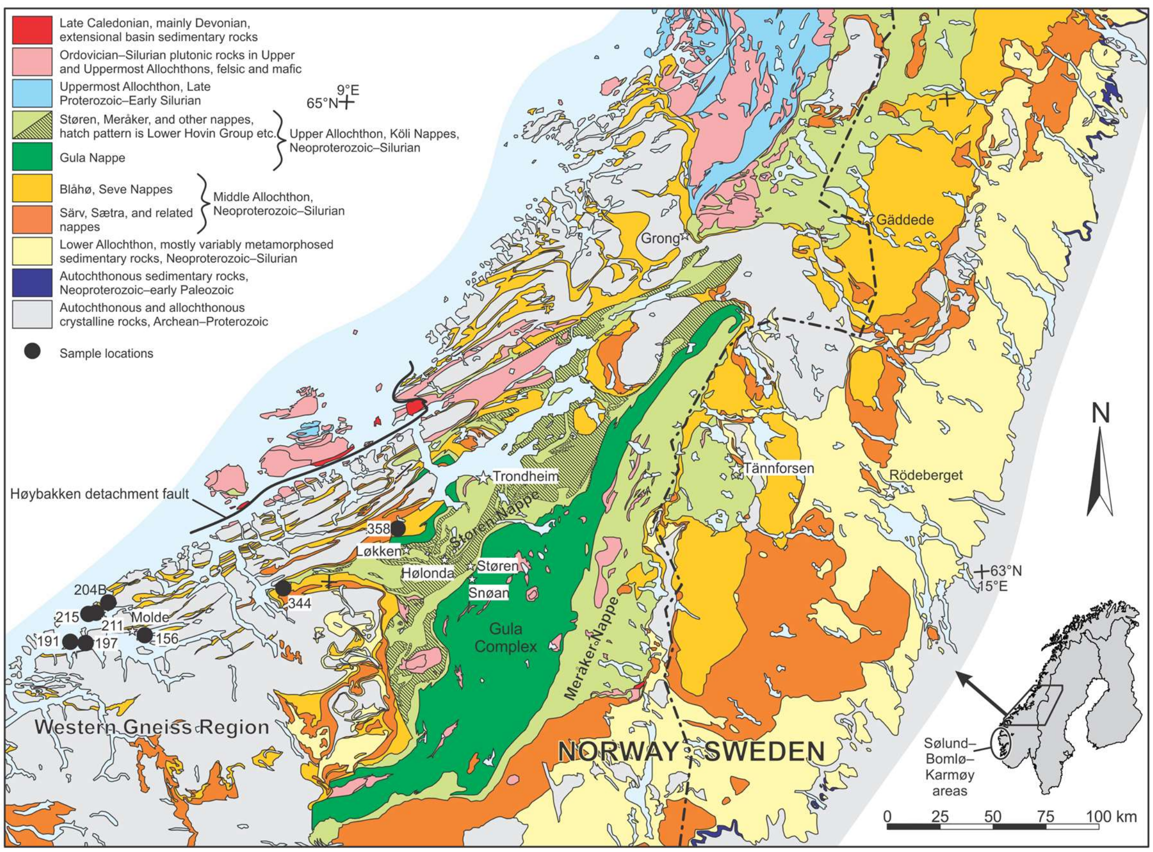

Figure 1. Tectonic map of the central Scandinavian Caledonides in Norway. The Blåhø Nappe (Middle Allochthon) occupies the darker yellow areas near the coast. Modified from Hollocher et al. (2016).

allochthon is, the more outboard from Baltica the source. The Lower and Middle Allochthons are largely from the margin of Baltica (Gee et al., 2008). The Upper Allochthon was derived from an oceanic arc complex that collided first with Laurentia before it was transferred onto Baltica in the Scandian collision (Gee et al., 2008). Lastly, the Uppermost Allochthon was originally a part of Laurentia itself (Gee et al., 2008). This study focuses on the Blåhø Nappe of the Middle Allochthon in central Norway, which is thought to have been from an Early Paleozoic volcanic arc presumed to have been in the Iapetus Ocean relatively near Baltica (Hollocher et al., 2015).

There was a complex history of metamorphism associated with the formation of the Scandinavian Caledonides. During the Scandian collision, oceanic crust subducted beneath the continental crust of Laurentia (Figure 2A), dragged downward by the weight of the cold, dense, sinking Iapetan oceanic lithosphere. Behind the subducting oceanic crust was the continental crust of Baltica, which consequently was being pulled down as well. The deeply subducted rocks formed high-pressure, relatively low-temperature eclogite (i.e. high-pressure metamorphosed basalts consisting largely of the minerals garnet and omphacite). However, the oceanic lithosphere eventually broke off and sank deeper into the mantle (Figure 2B). Due to its low density, continental crust is much more buoyant than oceanic crust, so freed of the dense, sinking oceanic lithosphere, the subducted Baltican margin began to rise to the surface. Rising to lower pressure conditions, the eclogites were no longer stable, leading to recrystallization to lower-pressure, amphibolite facies metamorphic assemblages. Some remnant eclogite blocks remained relatively intact as boudins and blocks in the newly reequilibrated amphibolites, giving evidence of the earlier, higher pressure conditions.

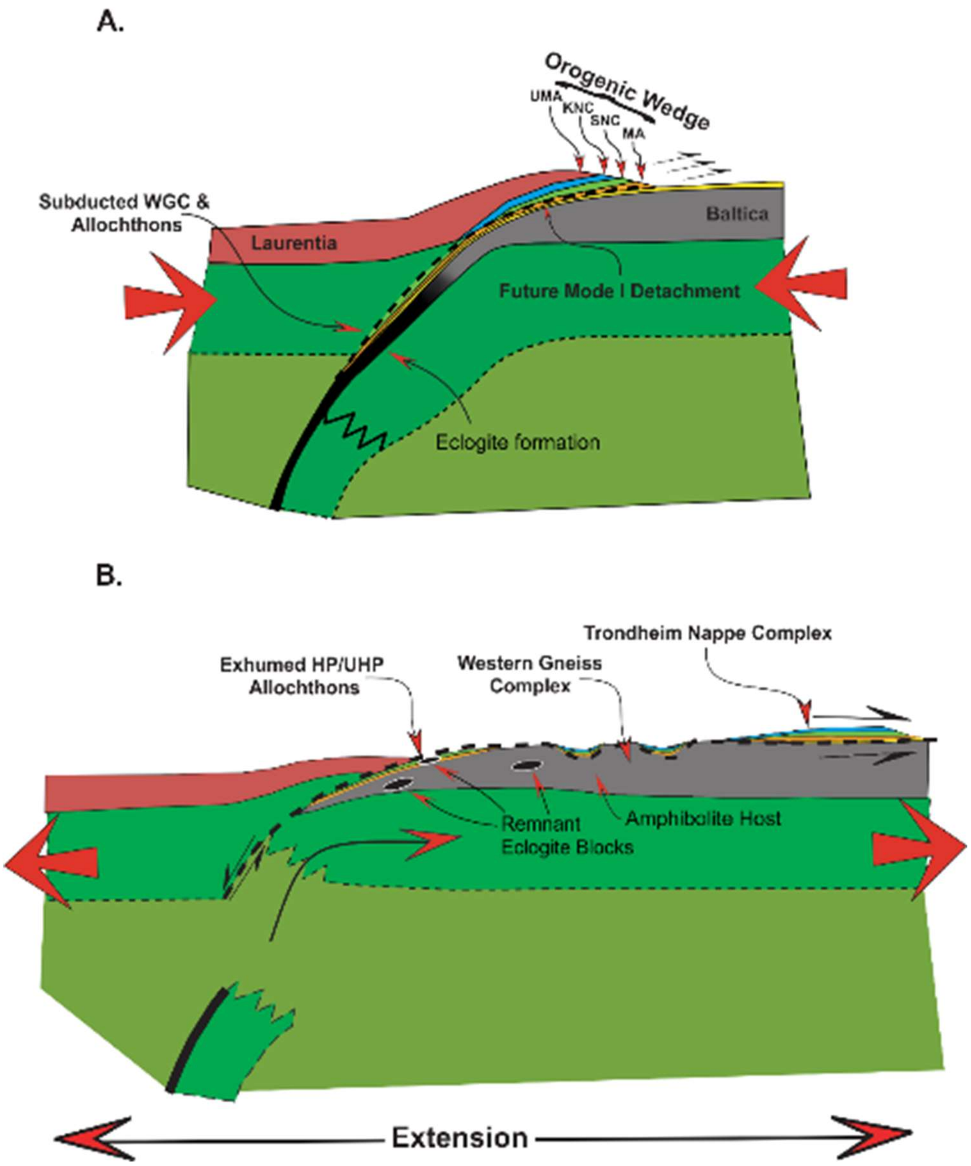

Figure 2. Tectonic model of the Scandinavian Caledonides, modified from Brueckner and Cuthbert (2013). A) During the initial Scandian collision (~435-405 Ma), the nappes begin to stack up, and Baltica began to subduct beneath Laurentia. B) Exhumation of the Western Gneiss Region, 405-390 Ma. After subducting, oceanic lithosphere broke away from Baltica, and felsic Baltican crust buoyantly rose to higher levels. Retrograde reequilibration during exhumation left sparse relict eclogite blocks (from HP/UHP conditions) in large volumes of amphibolite facies host rocks. UMA – Uppermost Allochthon; KNC – Koli Nappe complex (Upper Allochthon); SNC – Seve Nappe Complex (Middle Allochthon); MA – crystalline units of the Middle Allochthon. HP/UHP – high pressure/ultra-high pressure.

This study focuses on understanding the T-P path of the eclogites as they moved to lower T-P conditions to help reconstruct the tectonic history of this region, particularly with respect to the development of the Middle Allochthon. Mineral chemical compositions can be used to determine the metamorphic conditions of amphibolite formation because the chemical compositions of metamorphic minerals are sensitive to changes in pressure, temperature, and water content. Consequently, it is possible to determine temperature and pressure conditions recorded in the mineral assemblages of these rocks by analyzing the chemical composition of minerals sampled from that region and using that data for thermodynamic modeling (e.g. Terry et al., 2000; Eide and Lardeaux, 2002; McClellan, 2004; Hacker and Gans, 2005; Winter, 2010; Hollocher et al., 2015). The T-P conditions of eclogites in the Middle Allochthon (Figure 3A) have been relatively well-studied, but the lower T-P conditions for their amphibolite facies host rocks (Figure 3B) and related felsic gneisses (Figure 3C) are not well known.

PREVIOUS WORK

There has been considerable work in the Scandinavian Caledonides to try to understand the tectonic conditions and timing of Scandian orogenic activity. Geochronologic studies using the U-Pb radioactive decay series have been used to constrain the timing of the orogeny to between 426 and 390 Ma and to distinguish between distinct episodes of metamorphism (Krogh et al., 2004; Tucker et al., 2004). The timing of metamorphic episodes in the Scandian can be divided into Early, Middle, and Late stages. In the Early Scandian metamorphism, the collision between Baltica and Laurentia resulted in the formation of eclogites (~435 – 405 Ma, Figure 2A). During Middle Scandian metamorphism, uplift of the Baltican margin caused retrograding of most eclogites to amphibolite facies (~405 – 390 Ma, Figure 2B). Late Scandian metamorphism was a time of detachment faulting and sinistral shear in west-central Norway that led to continued uplift, and the filling of extensional basins with coarse clastic sediments (Robinson, 1995; Figure 1, youngest unit). There has also been tectonic modeling of the Scandian orogenic belt (Brueckner and Cuthbert, 2013) which explains how high-pressure rocks formed during the Scandian orogeny and how, later, remnant eclogite blocks and their retrograded hosts could return to the surface.

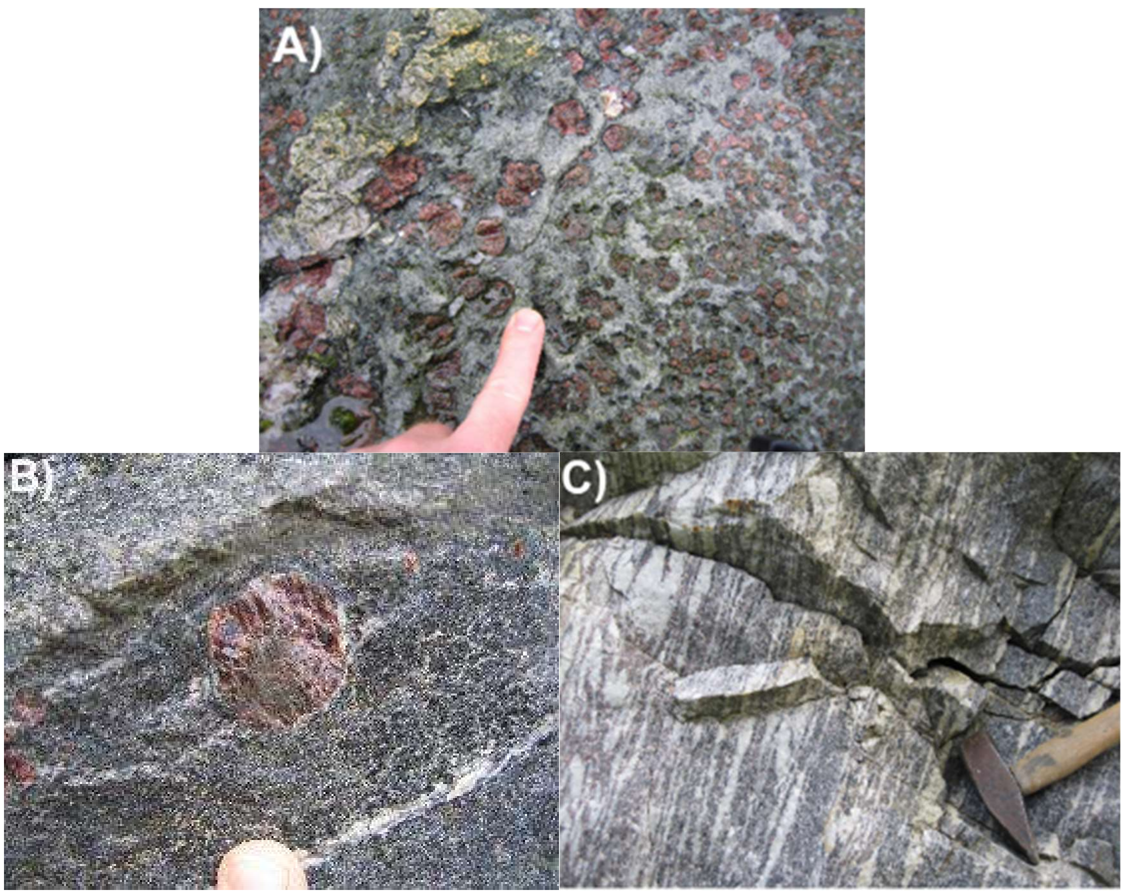

Figure 3. Field photos of sample sites in Norway. Photos by Kurt Hollocher.
A) Partially retrograded eclogite, with garnets and omphacite. Lower Allochthon, Røholmen Island between Haramsøy and Dryna mouth of Moldefiord. B) Amphibolite (inferred retrograded eclogite) with a large garnet. Middle Allochthon, Lepsøy. C) Felsic gneiss, with characteristic mineral layering indicative of partial melting. Middle Allochthon, north shore of Gossa.

Scandian, mostly amphibolite facies metamorphism in the Middle Allochthon has been studied in some detail in some aluminous schists to the east of my study area (McClellan, 2004; Hacker and Gans, 2005), and eclogites (Figure 3A) that occur mostly to the west and southwest (e.g. Krogh, 1980; Terry and Robinson, 2003; McClellan, 2004; Hacker and Gans, 2005). From garnet-biotite thermometry in the schists, it was estimated that during Late Scandian metamorphism, the temperature was approximately ~565°C deep within the Middle Allochthon with pressures of ~ 6 kbars (McClellan, 2004). The well-studied eclogites in the Middle Allochthon were metamorphosed at 600-800°C at 12 to 35 kbars (Hacker and Gans, 2005).

The Blåhø Nappe consists of igneous and sedimentary rocks that underwent medium-grade metamorphism to form gneisses, schists, calc-silicate rocks, marble, and amphibolites, and pegmatites from partial melting of felsic lithologies (Robinson and Hollocher, 2008). The aluminous schists mostly contain quartz, biotite, and garnet ± muscovite and kyanite (Robinson and Hollocher, 2008). The calcareous interlayered volcaniclastics commonly have potassium feldspar, biotite, diopside, epidote, and hornblende (Robinson and Hollocher, 2008). The amphibolites, which are the focus of this study, consist mainly of hornblende, and plagioclase ± quartz, garnet, epidote, and diopside (Robinson and Hollocher, 2008). The amphibolites also include partially retrograded and even fresh eclogite boudins in some places. Many of the amphibolites are coarse-grained and thoroughly recrystallized. The associated felsic gneisses, some of which were also examined in this study, mostly have small garnets, quartz, plagioclase, hornblende and biotite (Robinson and Hollocher, 2008). Some of the felsic gneisses have coarse, leucocratic layers, indicative of partial melting during metamorphism.

As is the case for other areas in the Middle and Lower Allochthons, many detailed petrological and geochronologic studies of the Blåhø Nappe have focused on eclogites (e.g. Terry et al., 2000; Krogh et al., 2004). Kyanite eclogites in an area regionally correlated with the Blåhø Nappe were described in detail by Terry et al. (2000). Little geochronologic work has been done on the Blåhø Nappe except for the dating of Scandian pegmatites (Tucker et al., 2004), and crystallization ages of eclogites (Krogh et al., 2004). Radiometric dating of one eclogite in the Blåhø Nappe has yielded metamorphic dates of 415 ± 2 Ma, with an overprinting of amphibolite facies metamorphism at ~410 Ma (Krogh et al., 2004). However, the temperature and pressure conditions of amphibolite facies metamorphism of the Blåhø Nappe, that makes up the vast majority of it, have yet to have detailed petrographic analyses.

There have been several studies of the Upper Allochthon in which mineral assemblages and compositions have been used to determine temperature and pressure conditions of metamorphism (e.g. Eide and Lardeaux, 2002; McClellan, 2004; Hacker and Gans, 2005; and Hollocher et al., 2015). During Early Scandian metamorphism, parts of the Upper Allochthon were metamorphosed to 550-600°C at 8-10 kbars (Hacker and Gans, 2005) whereas garnet-biotite thermometry yielded temperatures of ~495°C at ~ 6 kbars for Mid-to-Late Scandian metamorphism (McClellan, 2004). There are no known eclogites in the Upper Allochthon, but a relict glaucophane-bearing assemblage was found and associated with early Scandian or pre-Scandian metamorphism (Eide and Lardeaux, 2002).

FOCUS OF RESEARCH

This study aims to analyze the petrology and mineral compositions of Blåhø Nappe amphibolites (Figure 3B) and related felsic gneisses (Figure 3C) and to determine their recrystallization conditions. While the Blåhø Nappe has been examined in detail in the field (e.g. Robinson and Hollocher, 2008), most studies have focused on radiometric dating of pegmatites (e.g. Tucker et al., 2004) and petrology and radiometric dating of eclogites (e.g. Terry et al. 2000). There has been almost nothing published specifically about the temperature and pressure conditions of Blåhø Nappe amphibolites and felsic gneisses during Scandian metamorphism, so petrographic analyses of Blåhø Nappe samples will explore aspects of the Scandian tectonic history that have not yet been characterized.

Studying the mineral assemblages and compositions of Blåhø Nappe samples may be used to help constrain the temperature and pressure conditions of these rocks during Mid-to-Late Scandian metamorphism, during which eclogite facies rocks retrograded to amphibolites. To make thermodynamic models, mineral assemblages and textures were characterized using optical microscopy, backscattered electron microscopy, and quantitative analyses of mineral compositions were performed via standards-based energy-dispersive x-ray spectroscopy. From these, thermodynamic models were run to determine the likely conditions of amphibolite facies recrystallization, which will then be compared to regional data for eclogites.

METHODS

In this study, the methodology was very similar to that of Hollocher et al. (2015). The rocks examined from the study area are mainly amphibolites and felsic gneisses that are interpreted to have been recrystallized from higher-grade T-P conditions. 41 samples that had been collected by Professor Hollocher were selected from different areas of the Blåhø Nappe, and thin sections were made of them. The 41 samples are from a wide geographic range to make possible regional interpretations of the amphibolite facies recrystallization conditions. These samples were cut into thin sections by using water-cooled diamond saws to cut the rock into blocks the size of a microscope slide and about one centimeter thick, then thin polished sections were made and examined.

A total of 23 thin sections were observed in detail (see Table 1, Appendix 1). Most of the rocks examined were amphibolites, with assemblages dominated by plagioclase, amphibole, and diopside. Other major phases observed were garnet, biotite, epidote, and quartz. Several samples contained titanite, as well. Of the samples cut into thin-sections, eight were analyzed in detail: seven amphibolites (NOR-191, 197A, 204B, 211, 215, 344, and 358), and one felsic gneiss (NOR-156).

A petrographic microscope was used to assess mineral assemblages and textures in the samples. On petrographic microscopes, two different types of light settings (plane, cross-polarized) were used in tandem to do such qualitative studies. Plane light mode was generally used for assessing the mineral phases present in the section. Cross-polarized light was used to confirm the identity of minerals using characteristics such as mineral birefringence. Additionally, compositional zoning across the minerals (mainly epidote, plagioclase, and diopside, as well as some amphiboles) was observed using cross-polarized light. This compositional zoning was apparent by variations in birefringence across a single grain. For example, some epidotes had a sharply higher-order birefringence in the core, and plagioclase may also have cores and rims with distinctly different birefringence and extinction angles, in addition to the usual twinning. Lastly, petrographic microscopy was used to pick samples that seemed to offer the most promise of yielding usable results. These were mostly samples with little late-stage alteration of, for example, plagioclase to sericite.

Areas of focus were: 1) coarse assemblages with mineral phases representative of the thorough amphibolite facies recrystallization (i.e. re-equilibrated amphibolite matrix) 2) fine-grained recrystallized areas that may represent conditions of late Scandian deformation, and 3) symplectite textures clearly relict from retrograded eclogite, produced from the transition from high-T-P conditions (e.g. eclogite) to lower T-P conditions (e.g. amphibolite). In T-P space, the recrystallization from eclogite to amphibolite would, in thin-section, manifest as a range of mineral assemblages and textures from fresh eclogite (Figure 4A), partially retrograded eclogite (Figure 4B), and more retrograded eclogite (Figure 4C), to amphibolite with remnant eclogite retrograde textures (Figure 4D), and thoroughly recrystallized amphibolite (Figure 4E) assemblages that are the focus of this study.

Entire polished thin sections were scanned, selected areas were photographed, and the pictures served as location maps for backscattered electron microscopy. Back-scattered electron (BSE) imaging was used to select points for quantitative analysis due to its capabilities for high resolution imaging of minerals on the surface (i.e. top 2 microns) of the polished thin-sections. Grungy samples, such as samples with extensive sericite or abundant cracks and difficult to interpret disequilibrium textures, were not selected due to the increased potential for erroneous or uninterpretable results.

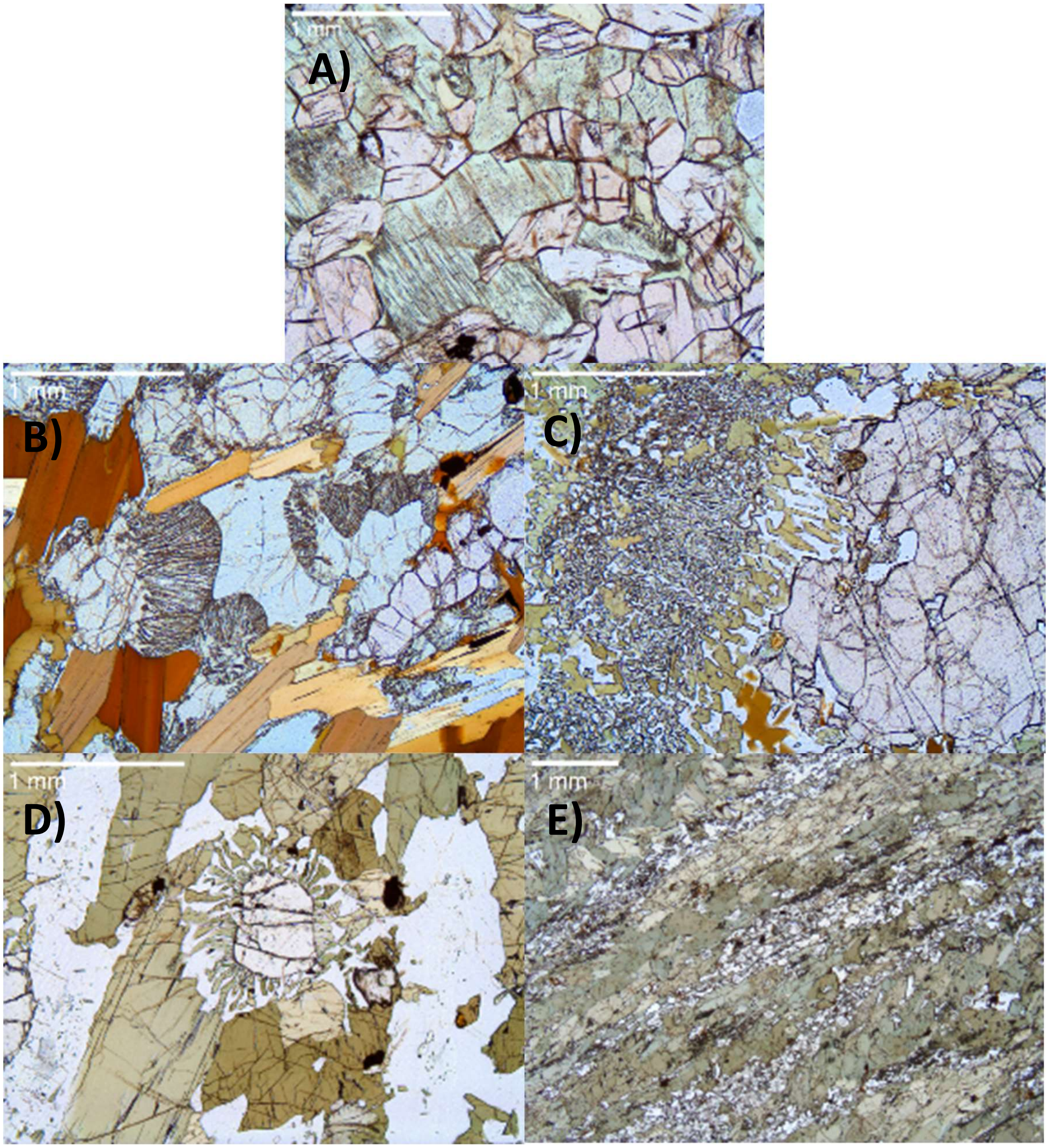

Figure 4. Thin section images (scale bars in upper left corner) in plane light, showing progression of retrograding from fresh eclogite to amphibolite. A) Fresh eclogite (Sample 025). B) Eclogite with plagioclase-augite symplectite partially replacing omphacite (Sample 017). C) Eclogite with plagioclase-augite symplectite entirely replacing omphacite, and hornblende-plagioclase symplectite partially replacing garnet (Sample 005). D) Almost completely recrystallized eclogite, now amphibolite, with hornblende-plagioclase symplectite surrounding garnet (Sample 204B). E) Thoroughly recrystallized amphibolite, with no relict eclogite or retrograde textures (Sample 344).

Entire polished thin sections were scanned, selected areas were photographed, and the pictures served as location maps for backscattered electron microscopy. Back-scattered electron (BSE) imaging was used to select points for quantitative analysis due to its capabilities for high resolution imaging of minerals on the surface (i.e. top 2 microns) of the polished thin-sections. Grungy samples, such as samples with extensive sericite or abundant cracks and difficult to interpret disequilibrium textures, were not selected due to the increased potential for erroneous or uninterpretable results. Additionally, X-Ray maps of elements of interest were made using energy-dispersive X-ray spectrometry (EDS) to distinguish minerals and textures that were not clear on BSE images. At least one BSE image was saved for each analyzed area to supplement the compositional analyses.

The Union College Zeiss EVO50XVP scanning electron microscope (SEM) was used for BSE imaging, but its primary purpose was to get quantitative compositional analyses of the sample. The initial parameters of the beam were a beam energy of 15 keV and a probe current of about 7 nA, adjusted as necessary. The stage was set to a Z-axis position of 37.9 mm for maximum X-ray signal on quartz and, once standardization began, magnification remained fixed, and all focusing was done using the stage Z-axis, not the beam magnet controls. Having chosen points for analysis, these were analyzed and recorded using standards-based EDS to provide quantitative information to be used in thermodynamic calculations. The analyzed points were chosen in hopes that the minerals in that area were representative of a set of metamorphic T-P conditions, and that the minerals came to be approximately in compositional equilibrium.

The EDS X-ray data were collected with a Bruker XFlash 6/30 silicon drift detector at a sensor temperature of -25°C, using a 0-60,000 count per second pulse processing range and typical count rate of around 35,000 counts per second. Before any quantitative analyses could be taken, it was necessary to calibrate the SEM to the silicate and oxide standards in the standard mount. Microbeam analytical methods on the SEM followed the standard-based EDS analytical methods described in Hollocher et al. (2015). The standards used were GKFS (microcline, K), px69 (augite, Mg), HEDE (hedenbergite, Fe), BHRH (rhodonite, Mn), PG721 (labradorite, Na), Tanz and Tanz 2 (identical tanzanite, Ca, Al, Si, oxygen), and Rut (rutile, Ti). The first part of the standardization process was calibrating the X-ray resolution and peak positions on polished copper in the standard mount. Then, the SEM spectra were calibrated to compositions on the chosen standard minerals. The analyzed minerals in thin section were almost all abundant silicates (amphibole, plagioclase, garnet, augite, epidote, biotite), but there were also a few *ad hoc* analyses of apatite, titanite, rutile, and sulfides. These included standardless determination of non-calibrated elements such as Cu, S, and P.

Following the methods described by Hollocher et al. (2015), the mineral analytical data were modified to be used in Perple_X thermodynamic modeling program (Connolly, 2009, Version 6.7.9). Modification was necessary because solution models of Perple_X were designed for exactly stoichiometric plagioclase, pyroxene, garnet, and epidote, and the solution models omit some commonly analyzed elements, such as titanium and manganese in pyroxene and amphibole. For this reason, our analyses had to be modified to fit the solution models, without distorting too much the mineral composition as represented by the remaining elements.

An example of the original analysis and the derived model compositions are provided in Table 2. First, the original mineral compositions (weight % oxides) were converted to cation proportions. Mn, K, and Ti are not included in many of the solution models used, and thus were removed from the mineral compositions. In hornblende and diopside, Mn was converted to Fe (Mn = Fe), and K was converted to Na = K. In plagioclase, K was removed as K-feldspar ($KAlSi_3O_8$). Ti was removed as $Ti_{-1}Al_{-2}(Mg,Fe)_1Si_2$ from hornblende and diopside (Mg and Fe in the analyzed mineral molar proportions). Fe^{3+} for amphibole was calculated following the method of Holland and Blundy (1994), whereas Fe^{3+} for diopside was calculated assuming 4 cations and 6 oxygens. These estimates of ferric iron had to be added to the mineral compositions because EDS analyses on the SEM cannot distinguish between ferric and ferrous iron.

Table 2. Example recalculation original mineral analyses in Sample 191, to modified analyses that fit the thermodynamic solution models, to the model rock composition (25% each in the mixture) given to Perple_X (weight %)

Sample	Original Mineral Compositions				Modified Mineral Compositions				Model Rock
	Amphibole	Plagioclase	Clinopyroxene	Garnet	Amphibole	Plagioclase	Clinopyroxene	Garnet	
Na_2O	2.30	7.12	1.31		2.70	7.26	1.30		2.82
MgO	10.35		11.52	5.91	10.53		11.42	5.82	6.94
Al_2O_3	14.22	25.94	5.76	21.57	14.53	26.08	5.51	22.02	17.03
SiO2	41.69	59.40	51.27	39.00	42.27	58.89	50.43	38.92	47.63
K_2O	0.37	0.03							
CaO	11.83	7.97	22.17	10.55	11.94	7.77	21.55	10.39	12.91
TiO_2	0.43		0.34						0.01
MnO	0.50		0.38	1.75					
FeO	16.69		9.17	21.43	12.70		6.30	22.85	10.46
Fe_2O3					5.33		3.49		2.21

After the above compositional changes were made, cation proportions were recalculated to cations per formula unit, then the mineral formulae were idealized to be stoichiometric. Plagioclase was recalculated from the average of four equivalent anorthite values: 1 – Na, Al – 1, 3 – Si, and Ca; diopside was normalized to a cation sum of 4 cations; and garnet was normalized to 3 large cations, 2 Al, and 3 Si. The new model compositions were then converted to oxide weight proportions (Table 2, column 2). Oxide weights were combined in appropriate model rock proportions (e.g. for this assemblage, 25:25:25:25 for amphibole, plagioclase, diopside, and garnet, respectively) to produce a model rock composition. Lastly, 0.01 % TiO_2 was added to the model rock composition to monitor the stability of rutile, ilmenite, and titanite.

The model rock compositions were run with Perple_X software to produce T-P isochemical sections (pseudosections). The solution models used were Pl(h) (plagioclase, Newton et al., 1981), cAmph(DP) (clinoamphibole, Diener et al., 2011), Cpx(HP) (clinopyroxene, Holland and Powell, 1996), Ep(HP11) (epidote, Holland and Powell, 2011), Gt(W) (garnet, White et al., 2014), and Bi(W) (biotite, White et al., 2014).

Mineral zoning and ranges of compositions within a single sample thin-section demonstrates that parts of each mineral may have been in equilibrium with different parts of the local assemblage at different times, and may represent different metamorphic conditions. For this reason, following the procedure of Hollocher et al. (2015), a large series of exploratory pseudosections were calculated using Perple X. Each pseudosection had a unique combination of analytical points from different mineral parts (such as cores or rims) and different mineral compositions to yield a model for its own distinct system composition. For example, the model determining the T-P conditions of the amphibolite-grade matrix in a sample would be in one unique run, whereas a model for potentially higher T-P conditions in a garnet symplectite within that same sample would be another separate run.

Even within the one small sample area, unique models may have to be made, as demonstrated, for example, by the recrystallized amphibolite matrix in Sample 191

(Figure 5). In that area, several analytical points were taken for each mineral. From the analytical points, mineral compositions were evaluated to determine whether or not there were significant differences in mineral compositions (mineral zoning). In the amphibolite matrix, the mineral assemblage consisted of hornblende (analytical points 01 – 04), plagioclase (points 05 – 07 and 13 – 14), and diopside (points 08 – 12). Analytical points 11 – 14 were omitted from thermodynamic modeling because they represent diopside (points 11 – 12) and plagioclase (point 13 – 14) in the (recrystallized) symplectite of the clinopyroxene, thus for that particular run they were inferred not to have been in equilibrium with the rest of the matrix.

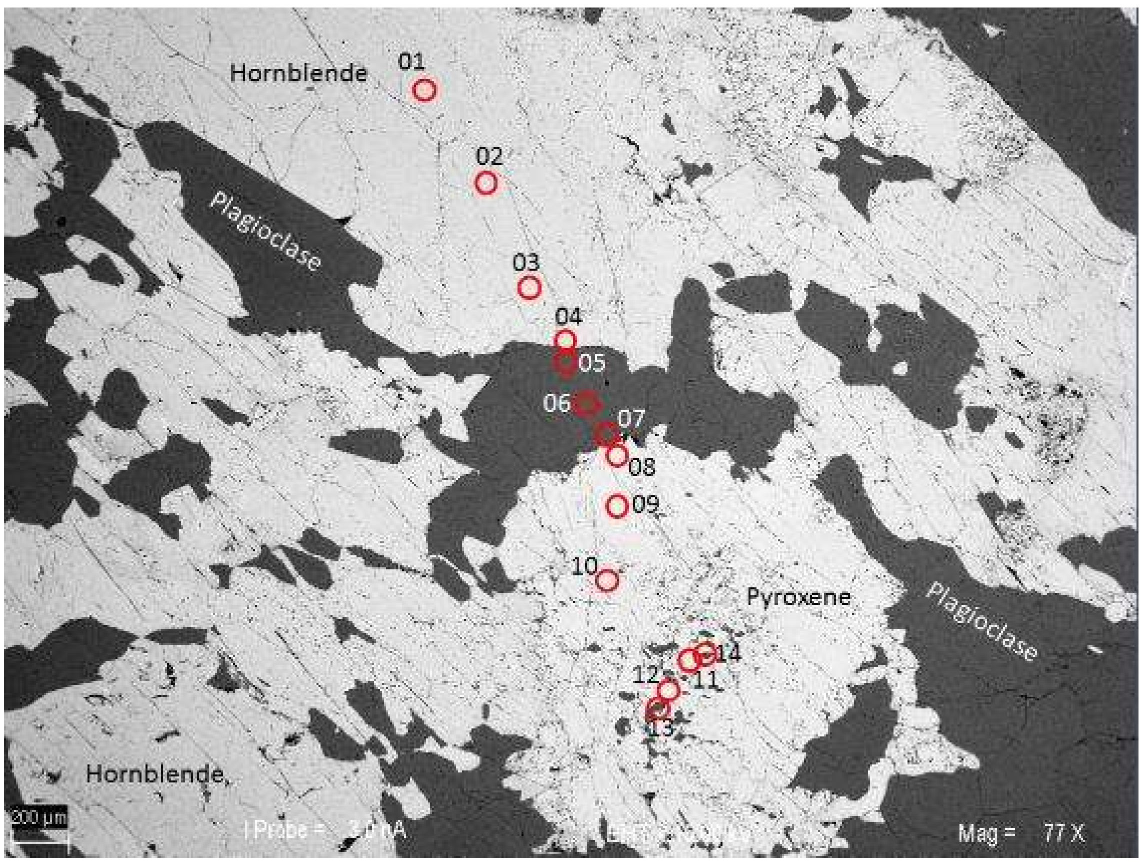

Figure 5. Analytical points in the thoroughly recrystallized augite-amphibolite matrix of Sample 191.

After excluding the symplectite compositions, the majority of the compositions for all of those matrix minerals were found to yield relatively consistent T-P estimates. However, the rims of diopside and amphibole (points 04 and 08, respectively) were somewhat different than the mineral interiors because both the diopside and hornblende rims had considerably less sodium and aluminum than the mineral interiors (Table 3). For this reason, two Perple_X model analytical runs were performed. The first included points in the interiors of amphibole (points 01 – 03), plagioclase (points 05 – 07), and diopside (points 09 – 10), whereas the second included points from the rims of amphibole (point 04), plagioclase (points 05 – 07), and diopside, (point 08).

Table 3. Comparison of mineral interior to rim analyses in Sample 191, matrix.

Phase	Clinopyroxene		Hornblende		Plagioclase	
	Interior	Rim	Interior	Rim	Interior	Rim
Na2O	1.60	1.04	2.61	2.26	8.10	7.92
MgO	11.42	12.52	13.14	13.46	-	-
Al2O3	7.05	4.75	13.91	12.87	25.07	25.11
SiO2	50.64	51.03	44.01	44.41	62.05	61.52
K2O	-	-	0.44	0.44	0.10	0.03
CaO	21.62	22.67	11.73	12.20	6.49	6.56
TiO2	0.32	0.42	1.03	1.38	-	-
MnO	0.22	0.19	0.17	0.22	-	-
FeO	7.56	7.36	11.75	11.92	-	-
Spectrum	191B-09	191B-08	191B-01	191B-04	191B-06	191B-07

Note: In clinopyroxene, K_2O was not analyzed, and in plagioclase, TiO_2, MnO, and FeO were not analyzed.

By matching the mineral proportions and compositions given to the model, with model results, the temperature and pressure conditions of the last equilibration of parts of the rock may be inferred. More mineral phases in each modeled assemblage were preferred, because more phases give more model constraints (Hollocher et al., 2015). For example, a rock made of one pyroxene has no constraints except for the large stability field for that sole pyroxene. Consequently, using assemblages with more phases allowed for more narrowly constrained T-P fields.

For each Perple_X model run, the results of the T-P pseudosection were exported into a 101 x 101 grid, 10,201 points. At each grid point the model results were assessed by: 1) comparing model phase compositions to actual compositions given to the model for several compositional criteria and 2) model phase proportions to phase proportions used in to calculate the model rock composition. If model phase compositions and phase proportions and actual compositions and phase proportions matched within a somewhat arbitrary uncertainty range in a particular T-P region, that region was considered to be the probable condition of last equilibration of that sample domain (a successful model, Hollocher et al., 2015).

An example of model results (Figure 6) is from mineral rims in the recrystallized amphibolite Sample 197, involving the phase plagioclase, amphibole, and diopside. In the T-P pseudosection, the model result table includes mineral modes (epidote, chlorite, zoisite, augite, amphibole, plagioclase, albite, titanite, rutile, ilmenite, and H_2O fluid), and phase compositions (plagioclase An, and Mg', Na, and Al in amphibole and augite). Modes of H_2O fluid and Fe-Ti oxides were ignored, and the Pl(h) plagioclase phase mode was added to the end member albite phase in the model, to yield a "total plagioclase" value. If actual values matched model values within some range at a point on the grid, that point is considered “good,” and marked with a 1. Points that do not match within that range are considered “bad,” and are given a zero. Dominant minerals in the modes were allowed a range of ±5% (e.g. 33% plagioclase ±5%). Minerals not observed in the thin section were allowed a range of 0 to 1% (e.g., epidote, which is not present in the analyzed assemblage). The range for phase compositions was typically 10-20% of the compositional value (e.g. 0.58 Mg’, ± 0.10) with a narrower range for anorthite content (± 0.05 An5). The sum of matching criteria (1s and 0s) is calculated for each grid point, and plotted as a T-P contour graph. According to this example model, the largest number of matching criteria (10 of 13 total) gave an estimate of recrystallization conditions of 560- 640°C, and 5.5 to at least 8 kbars (Figure 6).

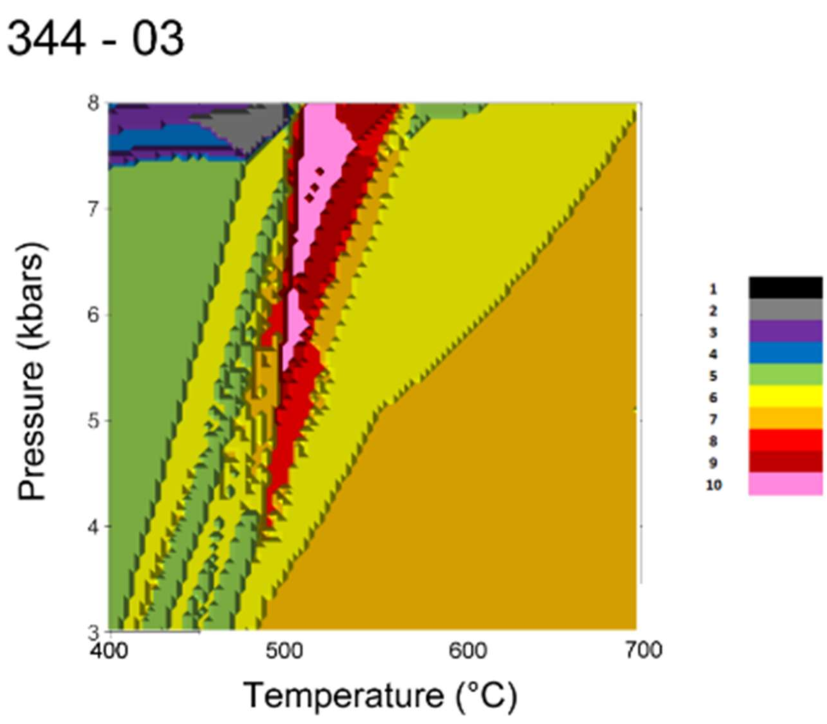

Figure 6. Thermodynamic model result, showing the number of model phase compositions and mode criteria that agreed with mineral compositions and phase proportions given initially to Perple_X (within an arbitrary uncertainty range, sample NOR-344). In this case, all 10 of the tested criteria matched, as described in the text, in the pink area at about 500–525°C and 5.5–8 kbars.

Of the numerous model runs for each sample, the "successful" models were compared with each other to determine if there were any consistent T-P conditions or trends within that sample. Results were also compared between samples to see if there was any regional consistency of T-P conditions. Ultimately, we are trying to determine if there is consistency of T-P conditions in many different samples, which would then give more confidence that the model conditions of amphibolite facies recrystallization were geologically meaningful.

PETROLOGY AND CRYSTAL CHEMISTRY

The main mineral phases observed and analyzed were hornblende, garnet, plagioclase, epidote, biotite, and diopside. Hornblende exists almost exclusively in matrix regions, making up the whole or bulk of the samples (Figure 4E), or in symplectites with plagioclase around garnet, with the exception of a few sparse inclusions in garnet or diopside (Figure 4D). Hornblende in the amphibolites ranges widely in composition, both from sample to sample as well as within a single sample (Figure 7). There were some samples with relatively homogenous matrix hornblende (e.g. Table 1), whereas others had some zoning (e.g. Figure 8).

Some of the pyroxenes are inclusion-free but with exsolution lamellae (Figure 9), but others have lots of plagioclase (and some hornblende) inclusions that look like they might be annealed symplectites exsolution lamellae or plagioclase-diopside symplectites, recrystallized from retrograde eclogites (Figure 10). Pyroxenes range between diopside (all diopside-bearing samples) and augite (few analyses, samples 204 and 215), and their compositions are not comparable to pyroxenes from eclogites except for the most Na-poor varieties (Figure 11), suggesting that they have reequilibrated from higher pressure.

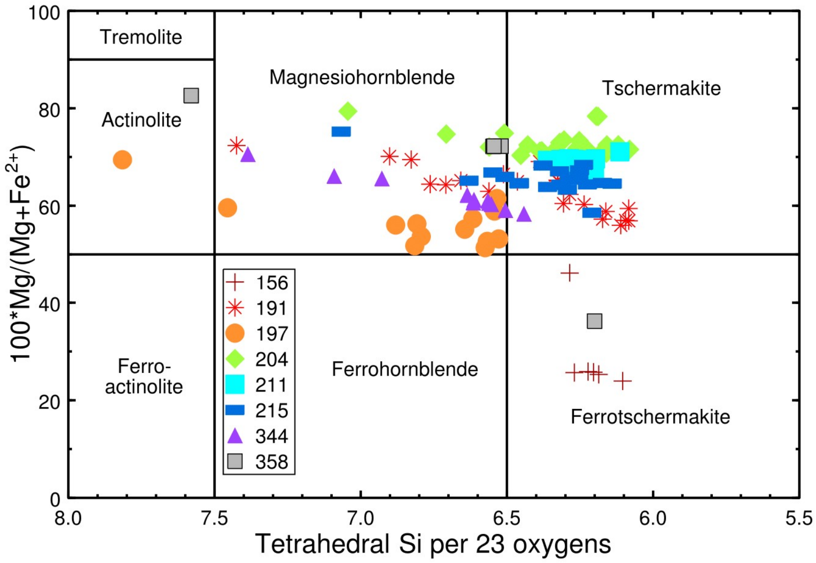

Figure 7. Classification of amphiboles in seven Blåhø Nappe amphibolites (191 – 358) and one felsic gneiss (156). Data show variability of hornblende composition, mostly having 100Mg/(Mg+Fe^{2+}) > 50. Even within a single sample, there is a range of hornblende compositions. The actinolite-bearing domains (NOR-197A) are very small, probably representing local, low-temperature re-equilibration in the presence of fluids.

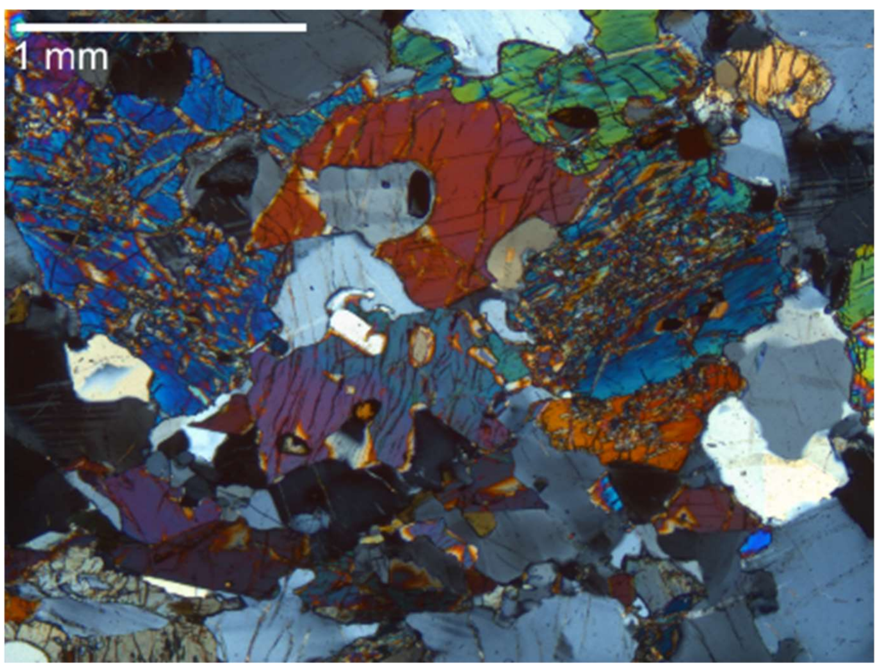

Figure 8. Subtle shifts in birefringence indicate hornblende zoning (center blue-to-purple grain NOR-215). Scale bar is shown in top-left corner.

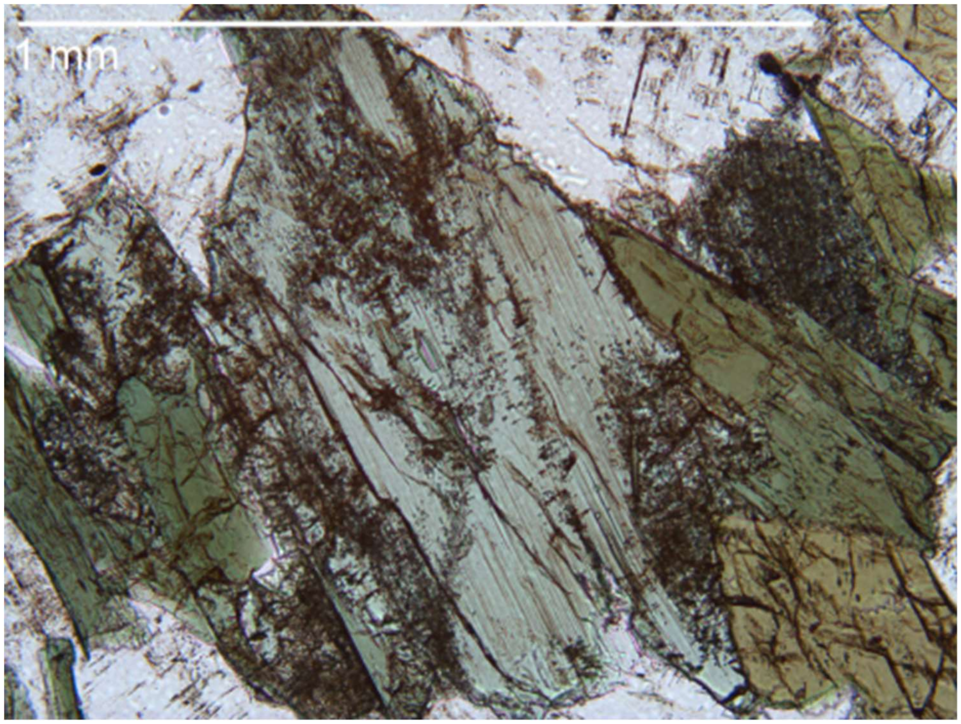

Figure 9. Diopside with plagioclase exsolution lamellae parallel to the length, but no larger plagioclase inclusions (NOR-191). Scale bar is shown in top left corner.

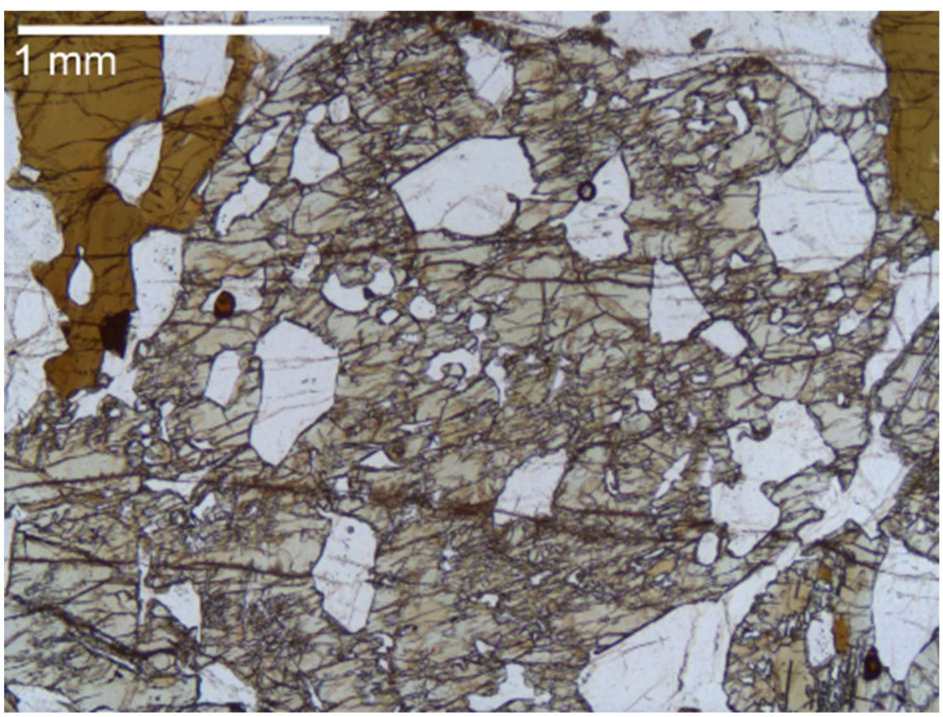

Figure 10. Diopside filled with irregular plagioclase inclusions (NOR-215), possibly recrystallized pyroxene-plagioclase symplectite retrograded from omphacite. Scale bar is shown in top left corner.

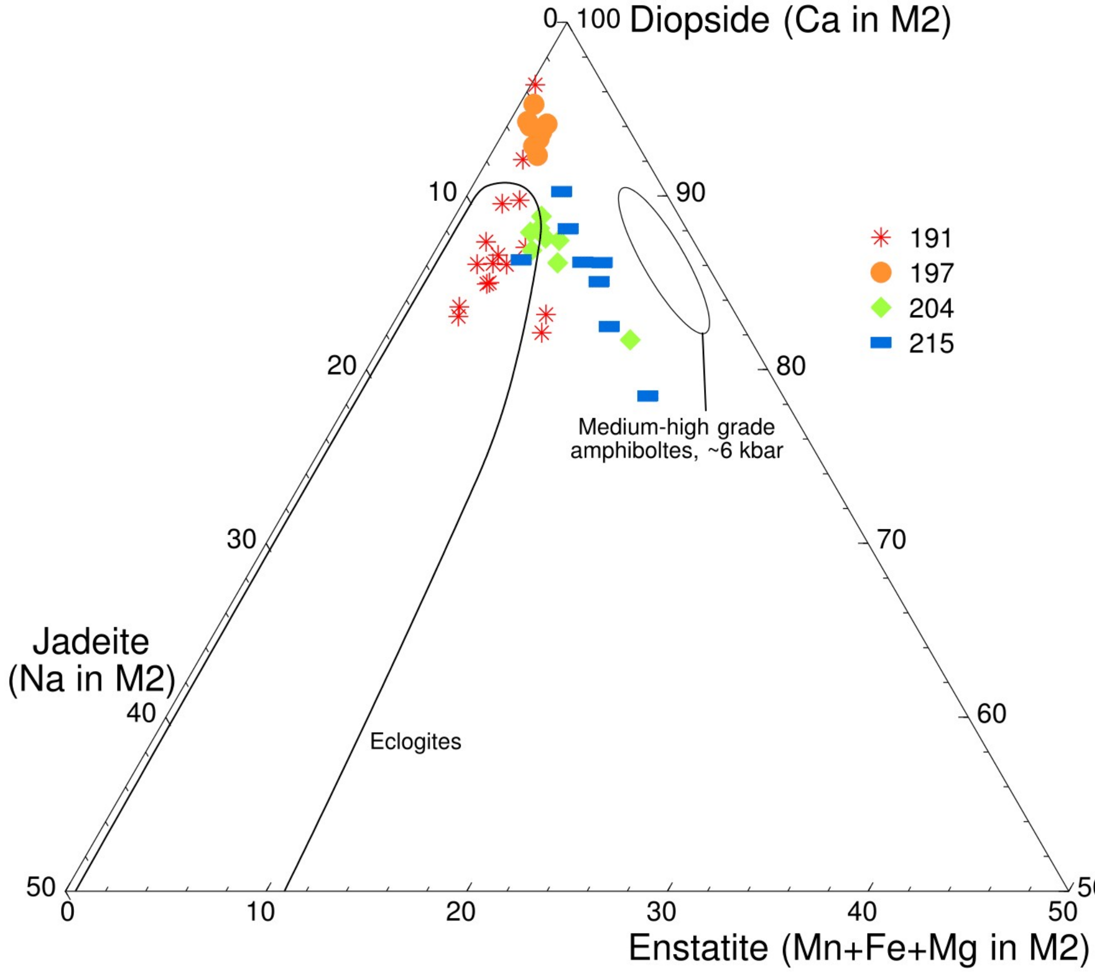

Figure 11. Chemical composition of pyroxenes in Blåhø Nappe amphibolites. All of the four samples plotted range between diopside and augite compositions. The eclogite field is based on data from Carswell et al.(1985), Cuthbert et al. (2000), and Hacker (2007). The 6 kbar field was made from data of Hollocher (1985).

Plagioclase was observed in matrix areas, symplectites around garnet, and as inclusions in diopside, garnet, and other materials. Many of the plagioclase crystals were extremely zoned (Figure 12). Garnet was relatively homogeneous, and generally associated with rimming symplectite textures, made of plagioclase and hornblende (e.g. Figure 4D). Compositionally, the garnets are all almandine and have similar compositions to garnets in some eclogites (Figure 13).

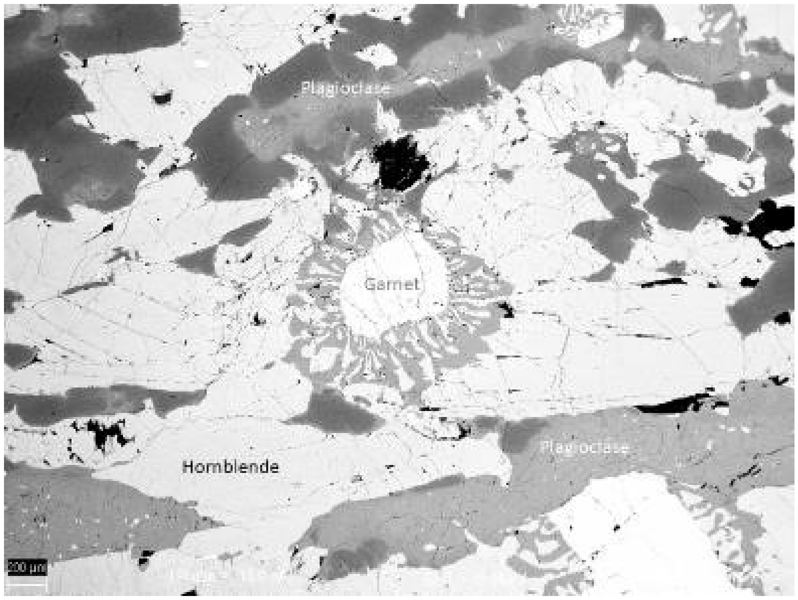

Figure 12. BSE image showing zoned plagioclase proximal to a hornblende-garnet symplectite surrounding garnet in NOR-204B. This profound plagioclase zoning in the matrix of the amphibolite (with sodic areas being darker, and calcic areas lighter) made interpreting possible equilibrium textures complicated. Note that the plagioclase in the symplectite is Ca-rich.

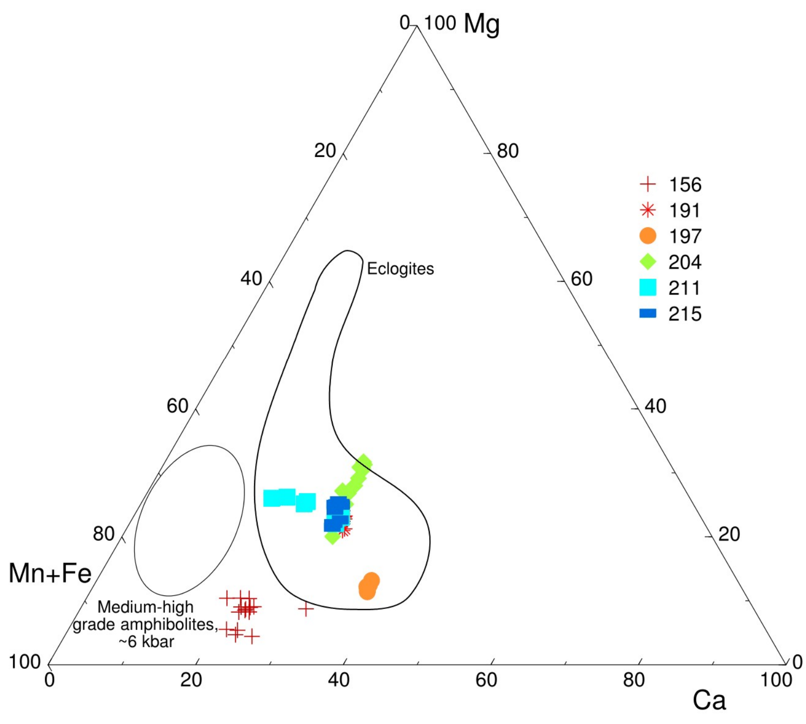

Figure 13. Chemical ternary of garnet in Blåhø Nappe amphibolites (191 – 215) and one felsic gneiss (156). These garnets are all almandine. The amphibolites have a relatively narrow range of garnet compositions. The felsic gneiss garnets are more Fe+Mn rich than those in the amphibolites, with lower Ca than all the amphibolites except NOR-211. The eclogite field is based on data from Carswell et al.(1985), Cuthbert et al. (2000), and Hacker (2007). The 6 kbar field was made from data of Hollocher (1985).

Other less abundant but significant minerals observed are epidote, biotite, and quartz. Epidote was not in many of the analyzed amphibolites, but many of the observed epidotes were zoned with higher birefringence in the cores (more Fe-rich, Figure 14). Biotite was more common than epidote in the amphibolites, and also was zoned with Mg-rich cores (e.g. Figure 15). The samples had varying amounts of alteration products, namely chlorite observed in samples with biotite (e.g. Figure 16) and sericite associated with plagioclase (e.g. Figure 17). Quartz was most abundant in the felsic gneisses (e.g. NOR-156), but it was also present in some of the amphibolite assemblages (e.g. NOR-197A and NOR-215; see Appendix 1).

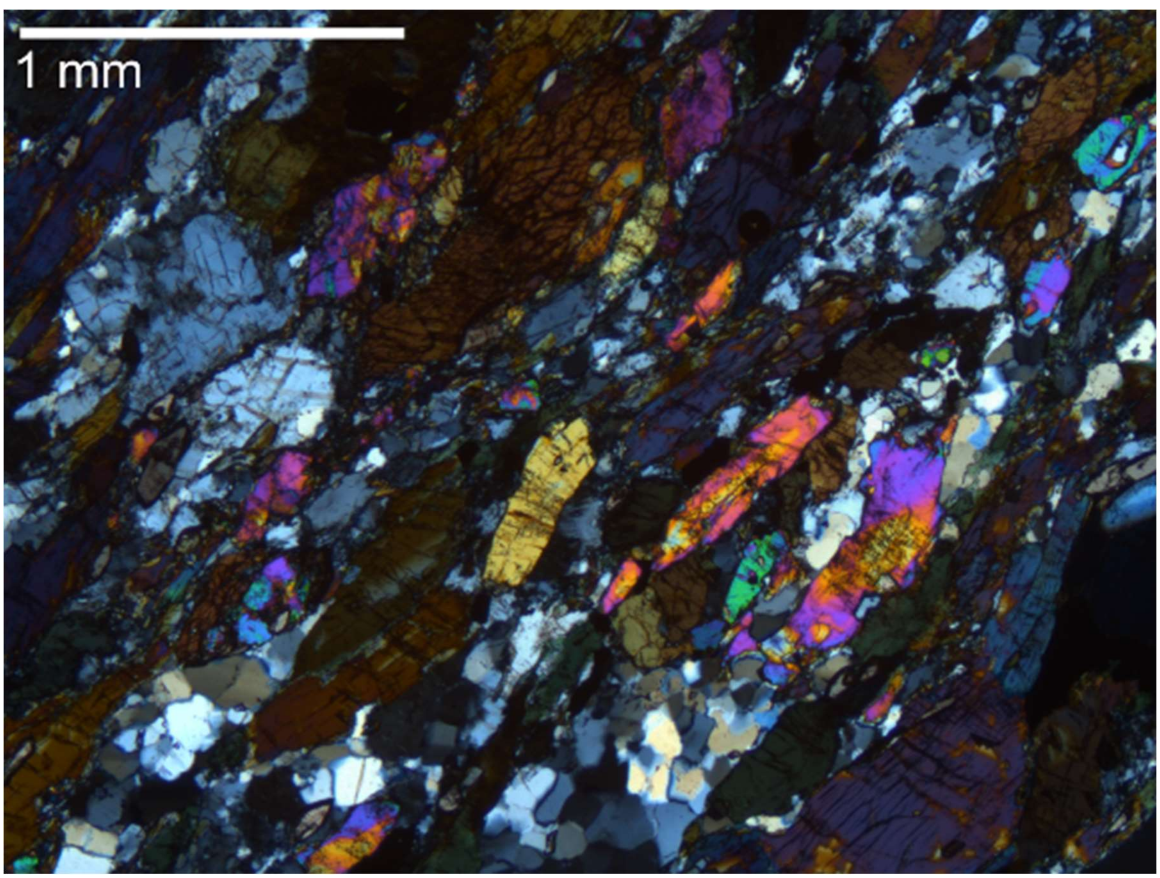

Figure 14. Zoned epidotes, many with bright cores (NOR-325). Scale bar shown in top-left corner.

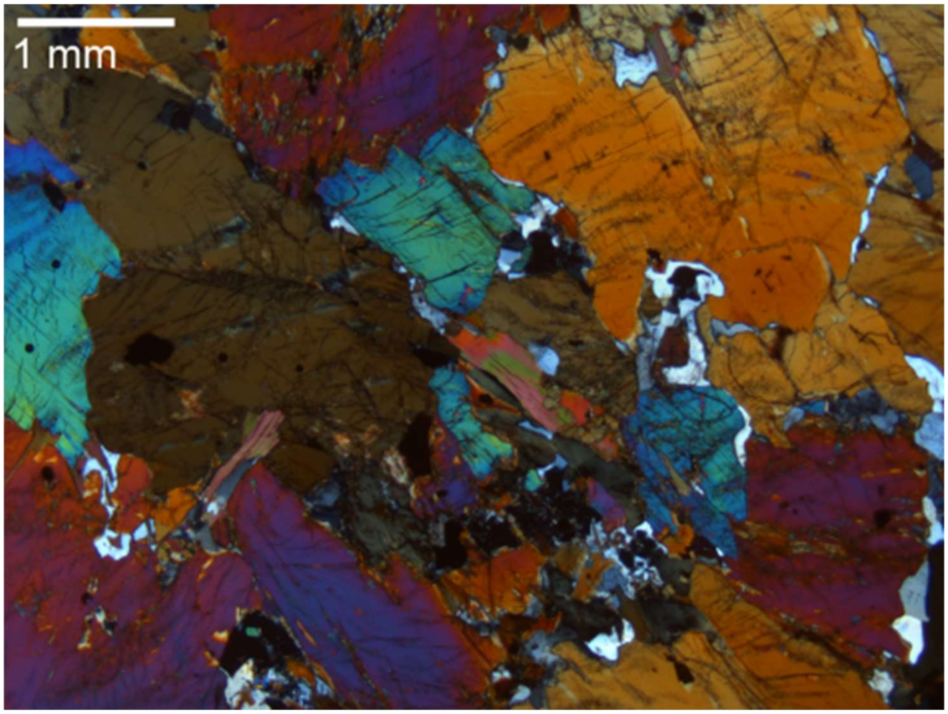

Figure 15. Zoned biotite, as well as more examples of hornblende zoning, both evident in the mineral birefringence and determined by spot analyses (NOR 211). Scale bar shown in top left corner.

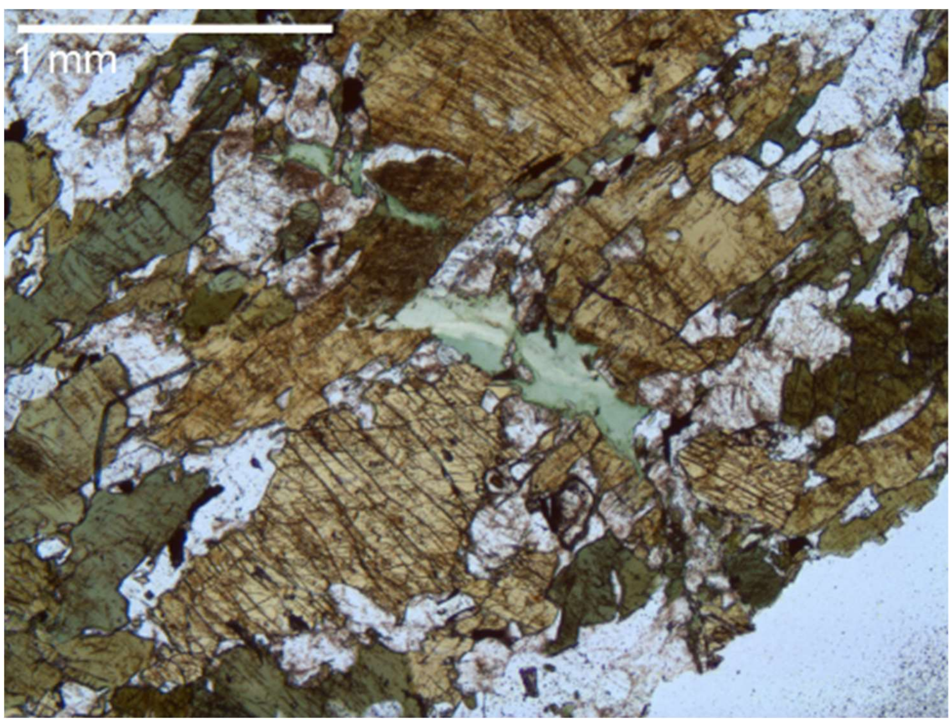

Figure 16. Chlorite, here interpreted to fill late extensional fractures that cut hornblende lineation that extends from upper-right to lower-left. Elsewhere, most chlorite is interpreted to be an alteration product associated with the mineral biotite (NOR-315). Scale bar is in the top left corner.

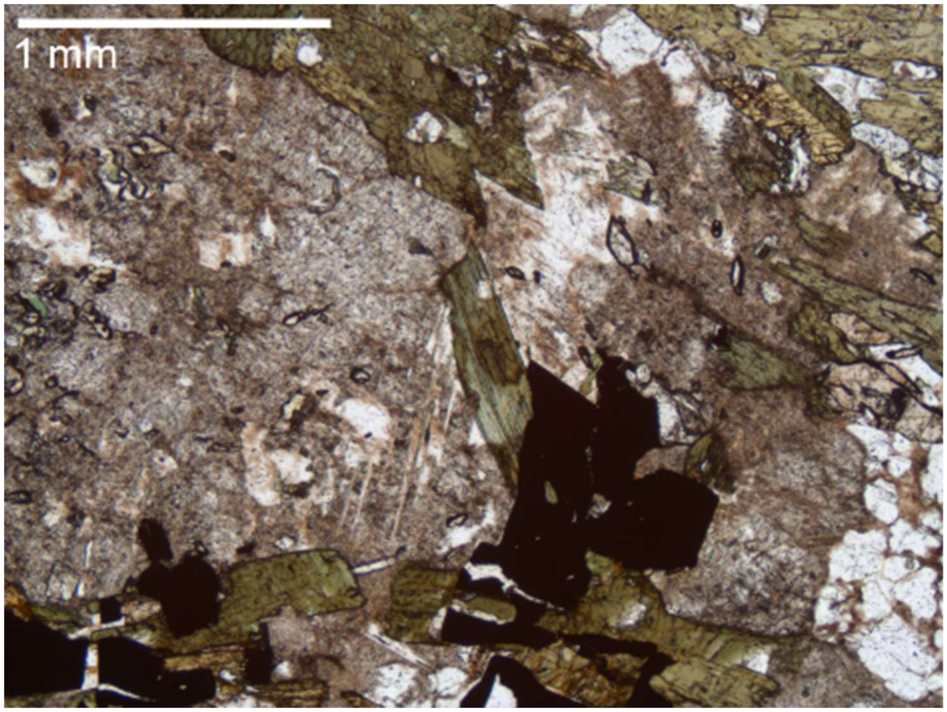

Figure 17. Sericite alteration was observed strictly in association with plagioclase (NOR-367). Samples like this were excluded from further work. Scale bar is in top left corner.

THERMODYNAMIC MODELING

The focus of thermodynamic modeling was on six amphibolite samples: NOR-191, 197A, 204B, 211, 215, and 344. Within each sample, between 5 and 10 Perple_X thermodynamic models were generated to determine consistency of T-P results, to determine if results consistently found one particular T-P region for amphibolite assemblage reequilibration, a logical range of T-P conditions, or no consistency of P-T regions among the different runs (see Table 4, Appendix 2). Within each sample, two types of domains were used to generate thermodynamic models in Perple_X: symplectite domains around garnet, presumably representing conditions between eclogite formation and matrix recrystallization in time and metamorphic T-P space, or amphibolite matrix, representing the end temperatures as the eclogites retrograded to amphibolite T-P conditions.

Two quantitatively-analyzed samples are omitted from the rest of this study: amphibolite NOR-358 and felsic gneiss NOR-156. Analytical difficulties caused mineral compositions in NOR-358 (weight % oxides) from EDS to be less accurate than that for other samples, with error values of ±4% rather than ±2%. Mineral compositions for the felsic gneiss are distinct from the amphibolites (Figure 7), and more felsic gneiss data would be needed to make geologically meaningful comparisons of metamorphic T-P conditions in felsic gneisses compared to amphibolites.

NOR-191

NOR-191 is an amphibolite with sparse garnet; only a single large and one small porphyroblast were observed in thin section, each surrounded by partially recrystallized hornblende-plagioclase symplectite rims. While epidote is present in this sample, the focus of the modeling was to determine the T-P conditions of the symplectites in the sample and the recrystallized amphibolite matrix. Zoning of the plagioclase in this sample resulted in inconsistency among some of the matrix models. The Perple_X run with the most matching compositional and modal criteria is 191-02 was chosen to be representative of re-equilibrated amphibolite matrix in this sample (Figure 18). Data from the area around the largest porphyroblast symplectite yielded a model with the most criteria, and was taken to represent the post-eclogite conditions (Figure 19).

NOR-197A

NOR-197A is a fine-grained, recrystallized amphibolite with only sparse, indistinct symplectite textures around garnet porphyroblasts. However, the focus of

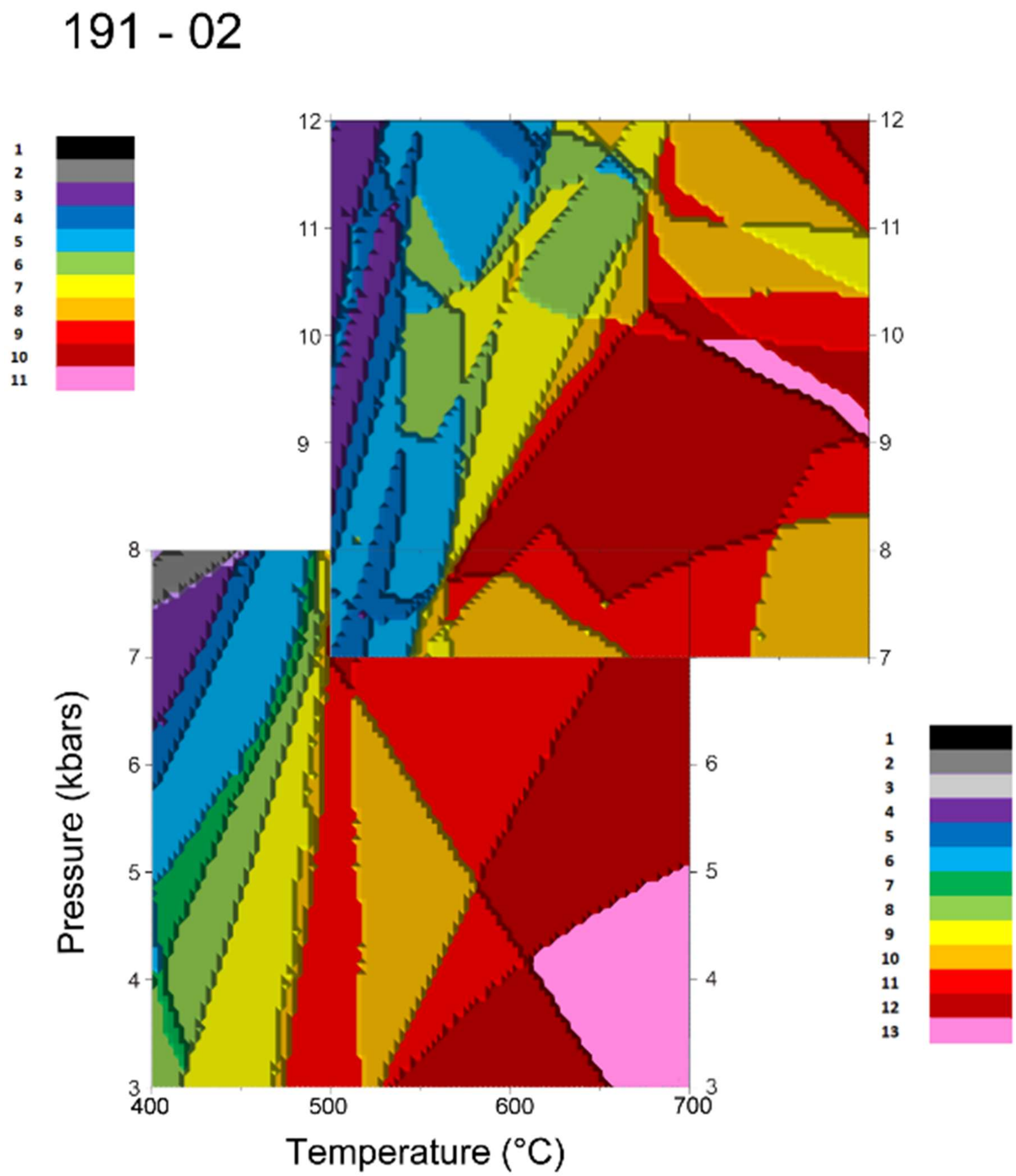

Figure 18. Perple_X thermodynamic model result for coarse matrix assemblage of amphibolite sample 191. The minerals input into the assemblage were plagioclase, amphibole, and clinopyroxene. There are 15 total criteria in the both the low-pressure and high-pressure sections. Pink represents the area with the most matching criteria, whereas black has the fewest.

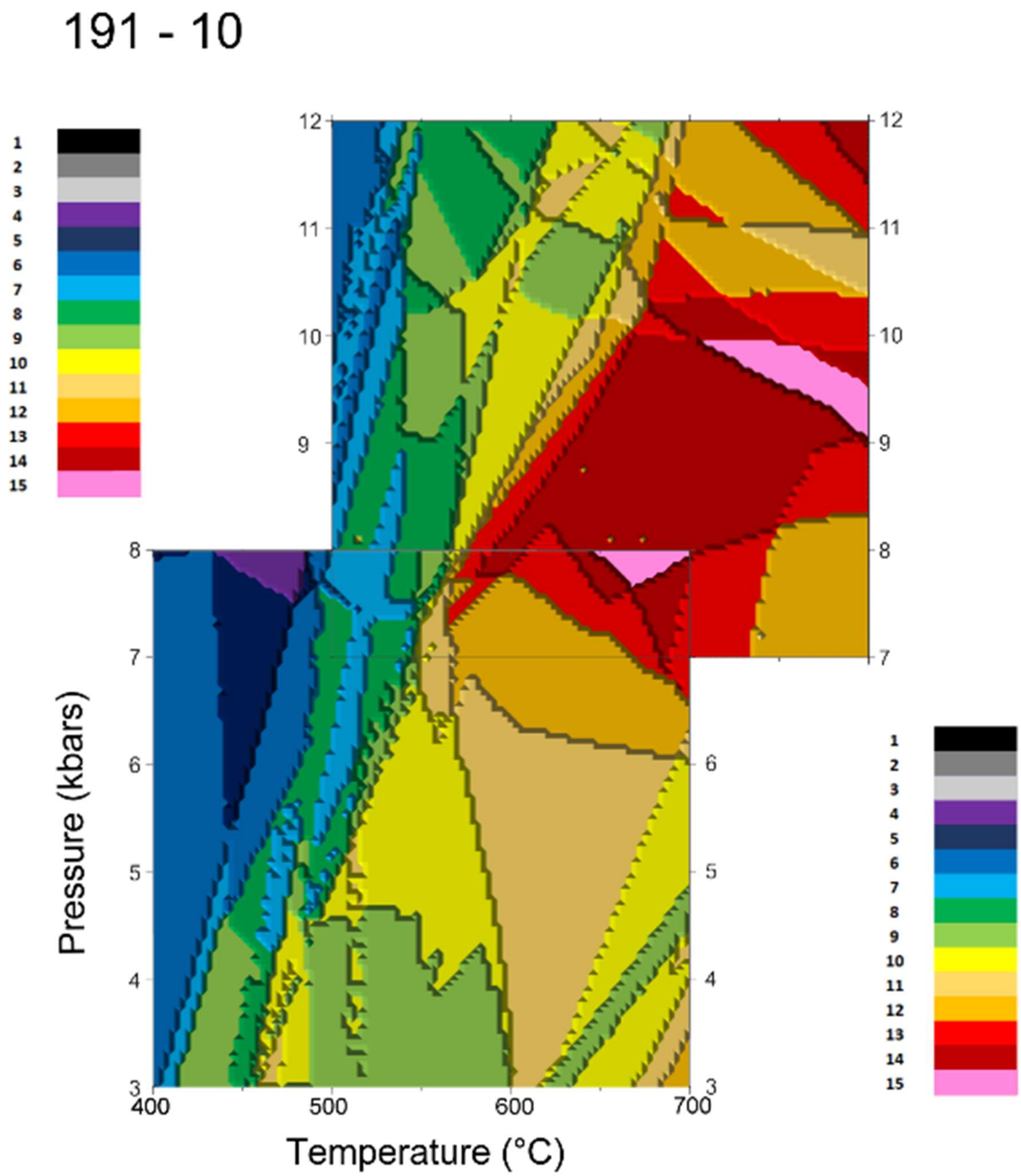

Figure 19. Perple_X thermodynamic model result for a garnet symplectite area in amphibolite sample 191. The minerals input into the assemblage include plagioclase, amphibole, and garnet. Pink represents the area with the most matching criteria, whereas black has the fewest. There are 17 total criteria in the low-pressure section, and 19 in the high-pressure section.

thermodynamic modeling for this sample was on the coarse-matrix, re-crystallized amphibolite rather than the remnant eclogite textures. Coarse matrix T-P results were somewhat consistent within the sample (Figures 20 and 21). More Perple_X runs will be needed to determine what T-P conditions are associated with the garnet symplectites. Some model rock compositions that could be run include 197A-01 and 197A-02 (Appendix 2).

NOR-204B

NOR-204B is a coarse-grained amphibolite with classic plagioclase-hornblende symplectites around garnet, but profound plagioclase zoning. Two Perple_X thermodynamic runs were made for garnet symplectites (204B-01, 204B-04), and the results of both were very similar, with T-P conditions of 700-800°C and 9.5 to 10.5 kbars. Only one of those symplectite runs, 204B-01 is discussed in this paper (Figure 22). The matrix of the amphibolite, however, was more complicated to determine possible equilibrium assemblages because of zoning. The thermodynamic models produced from the matrix were inconsistent. For this reason, only the best model for matrix composition – with the most criteria, and the most matches – is presented here (Figure 23).

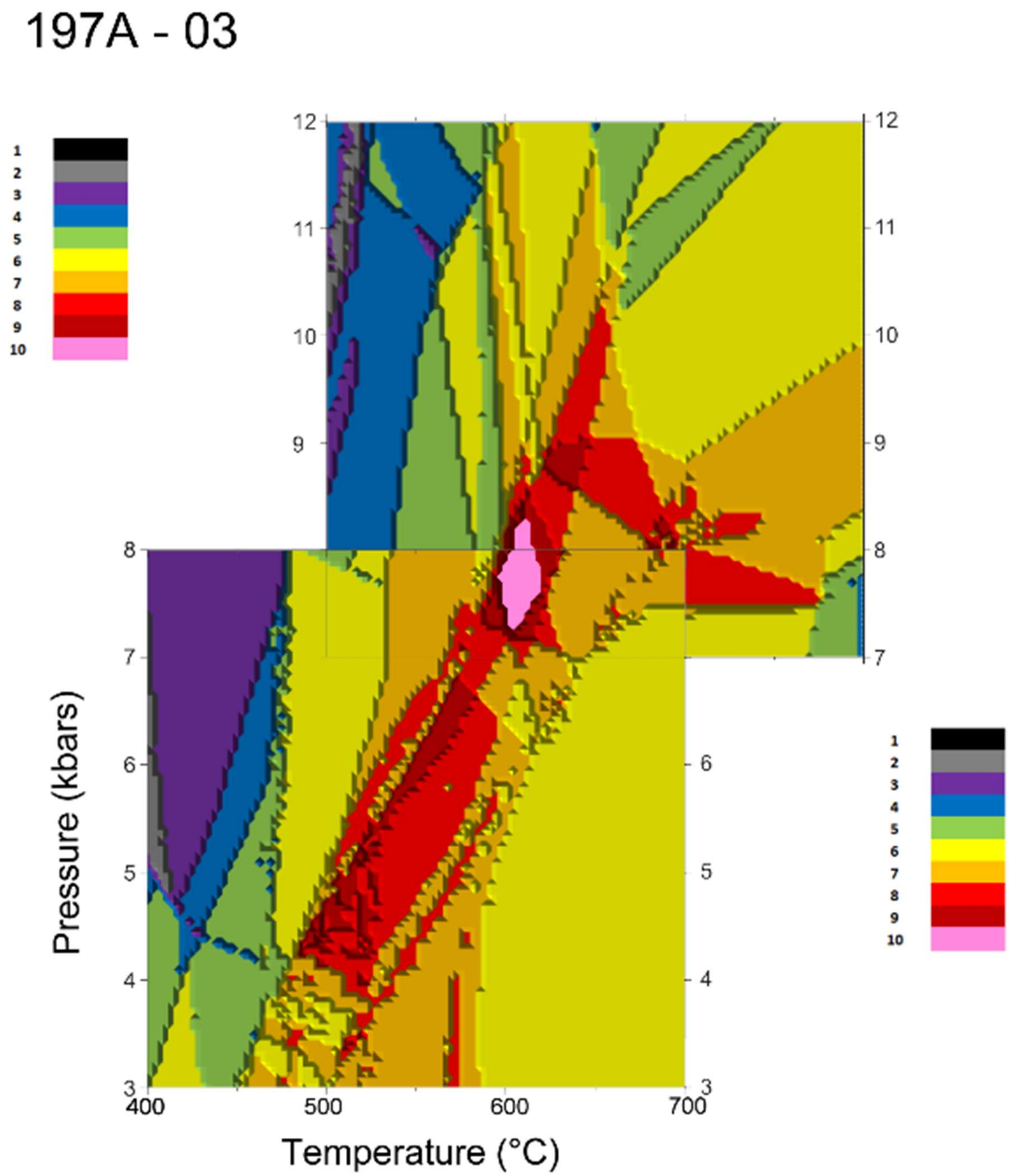

Figure 20. Perple_X thermodynamic model result for the coarse matrix assemblage of amphibolite sample 197A. The minerals input into the assemblage include, plagioclase, amphibole, and garnet. Pink represents the area with the most matching criteria in each section, whereas black has the fewest. There are 14 total criteria in both the low-pressure and high-pressure sections.

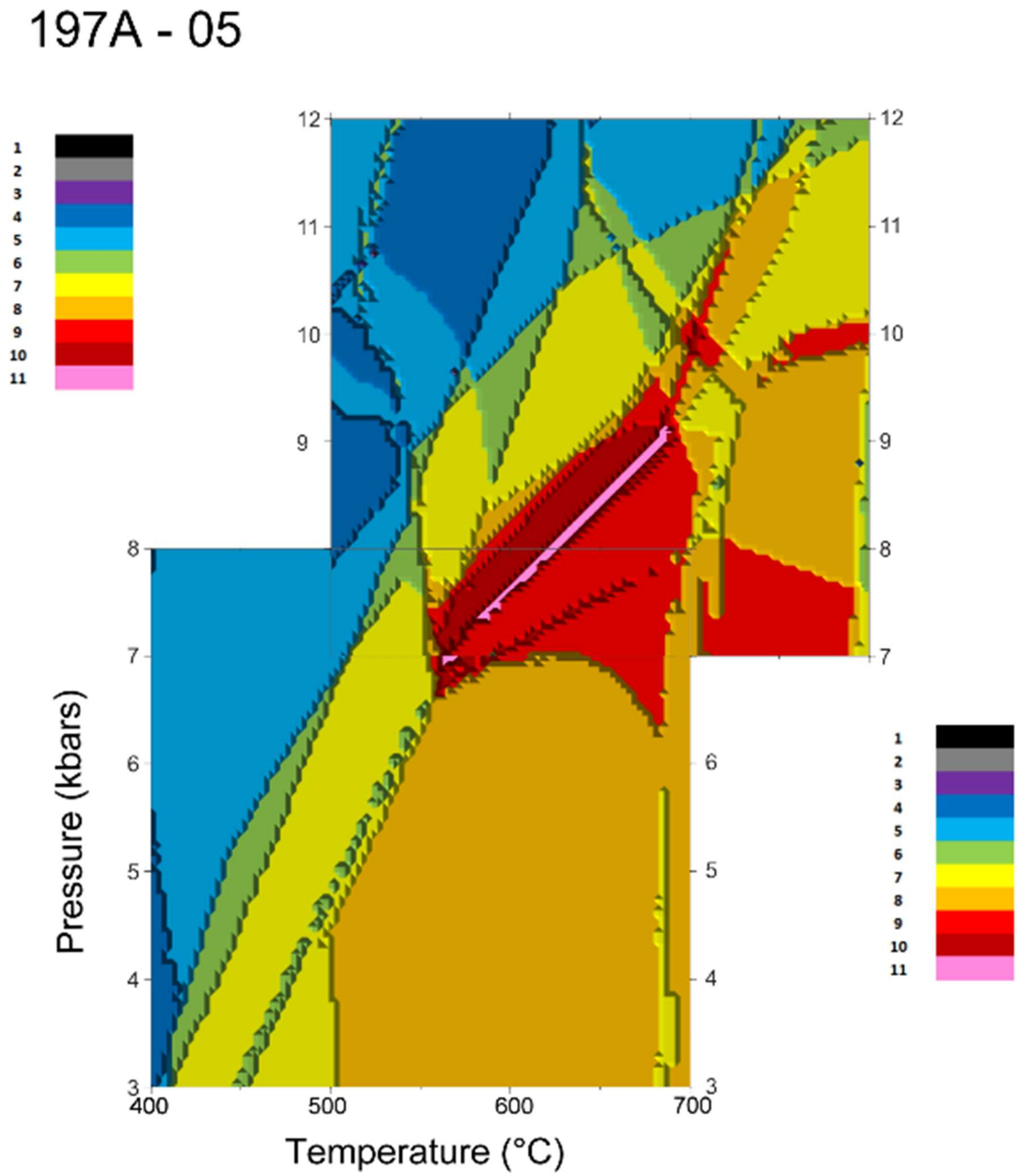

Figure 21. Perple_X thermodynamic model result for the matrix assemblage of amphibolite sample 197A. The minerals input into the assemblage include plagioclase, amphibole, and diopside. Pink represents the area with the most matching criteria in each section, whereas black has the fewest. There are 13 total criteria in the low-pressure section, and 14 in the high-pressure section.

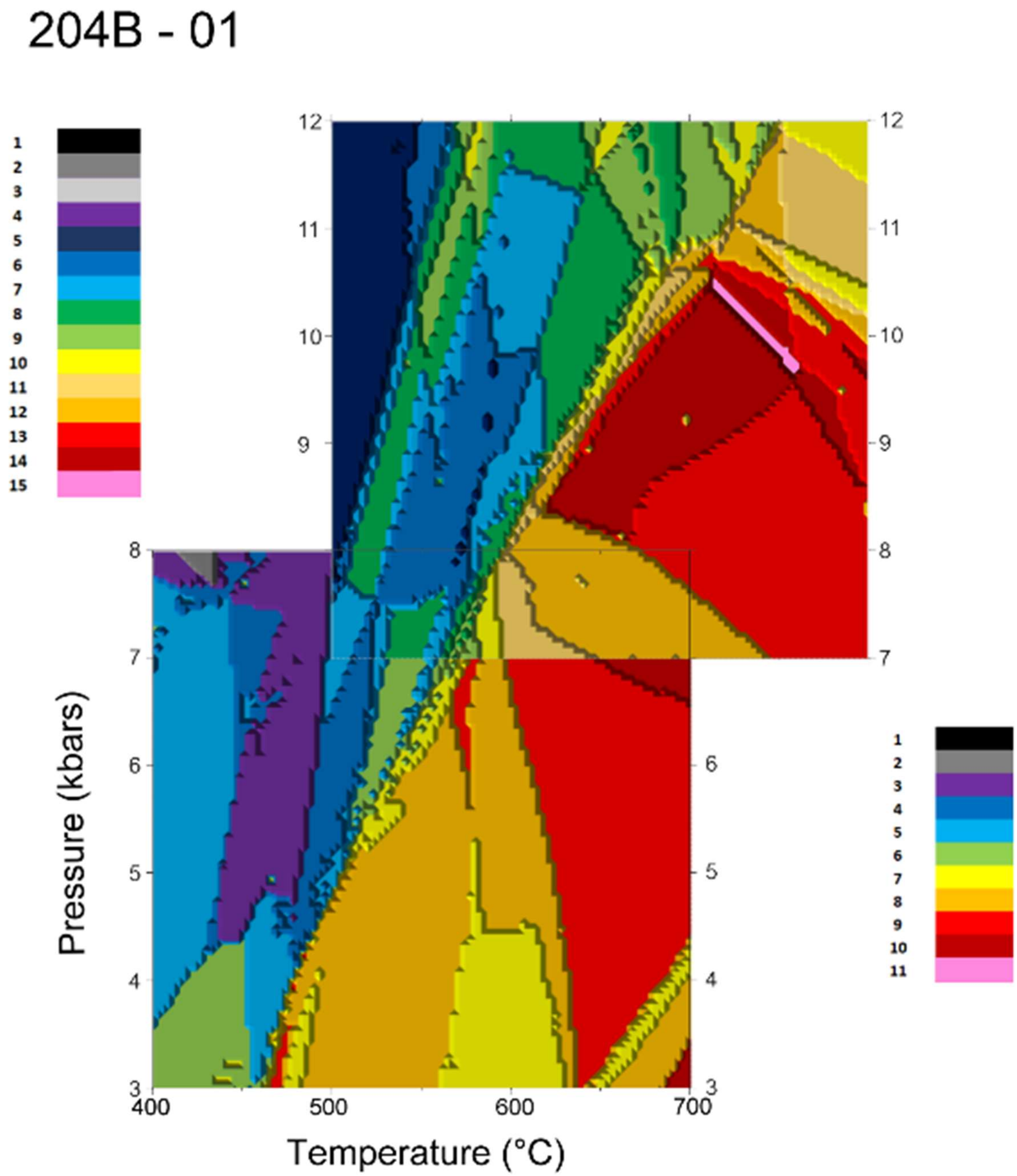

Figure 22. Perple_X thermodynamic model result for a garnet symplectite area in amphibolite sample 204B. The minerals input into the assemblage include plagioclase, amphibole, and garnet. Pink represents the area with the most matching criteria in each section, whereas black has the fewest. There are 16 total criteria in the low-pressure section, and 18 in the high-pressure section.

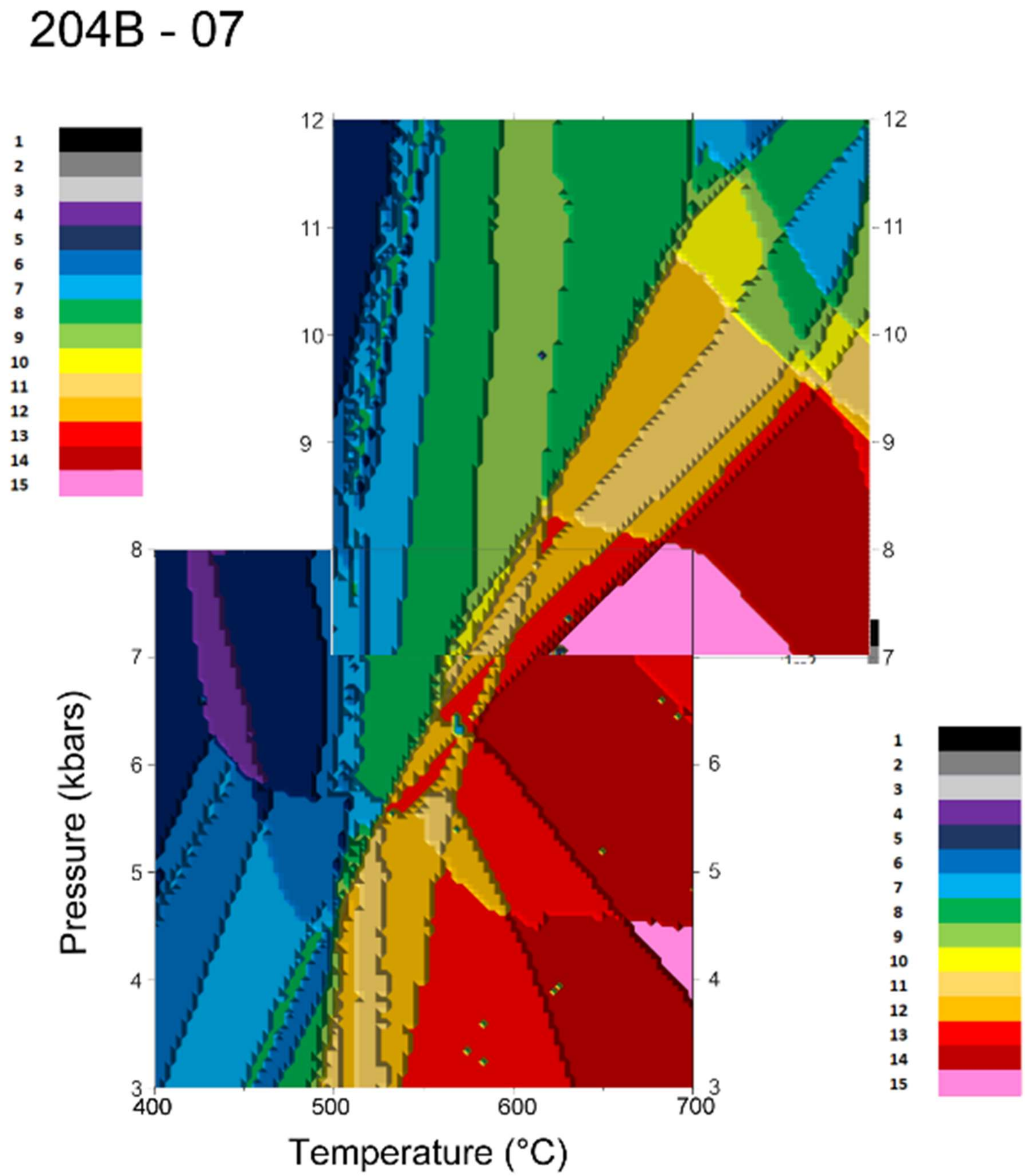

Figure 23. Perple_X thermodynamic model result for the coarse matrix assemblage of amphibolite sample 204B. The minerals input into the assemblage include plagioclase, amphibole, and garnet. Pink represents the area with the most matching criteria in each section, whereas black has the fewest. There are 15 total criteria in the low-pressure section, and 16 in the high-pressure section.

NOR-211

NOR-211 is a coarse-grained amphibolite with biotite and garnet in addition to the hornblende and plagioclase. There are no symplectites, but the highly anhedral garnets are surrounded by thin plagioclase moats. This rock was examined with the intention of seeing how minerals such as biotite may affect the thermodynamic models. Several models for the T-P conditions of the garnet-moat plagioclase-hornblende composition were examined, but only one of them yielded a single, narrow range of T-P conditions that could be compared to other samples (Figure 24). This sample is the only amphibolite with biotite included in the matrix model-rock composition (Figure 25).

NOR-215

NOR-215 is a recrystallized amphibolite with quartz, anhedral garnet, and inclusion-rich diopside. The garnets are largely surrounded by narrow plagioclase moats. A single thermodynamic model was made using the recrystallized plagioclase-diopside symplectite textures (Figure 26). Within plagioclase moats surrounding the sample, there were several different sizes of garnets and hornblende inclusions, which were analyzed. Thermodynamic models of smaller hornblende inclusions (Figure 27) and larger hornblende inclusions in a plagioclase moat around a garnet (Figure 28) yield comparable T-P conditions, demonstrating consistency for the remnant-eclogite conditions within the sample. For the coarse matrix, the Perple_X thermodynamic run with the most matching criteria was taken to be the representative model for this sample (Figure 29).

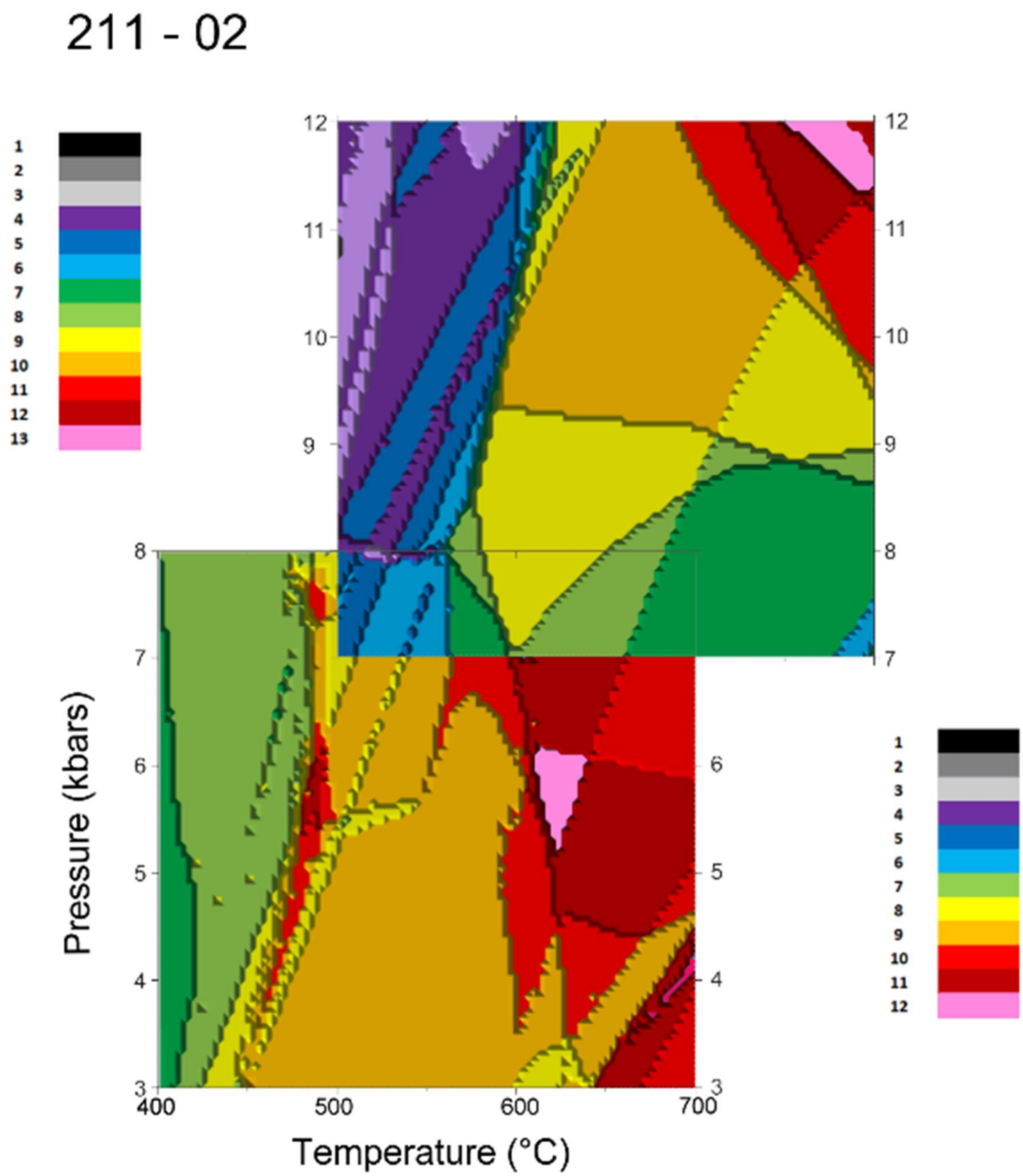

Figure 24. Perple_X thermodynamic model result for a symplectite assemblage of amphibolite sample 211, including the edges of the amphibole but not the interiors. The minerals input into the assemblage include plagioclase, amphibole, and garnet. There are 17 total criteria in the low-pressure section, and 15 in the high-pressure section.

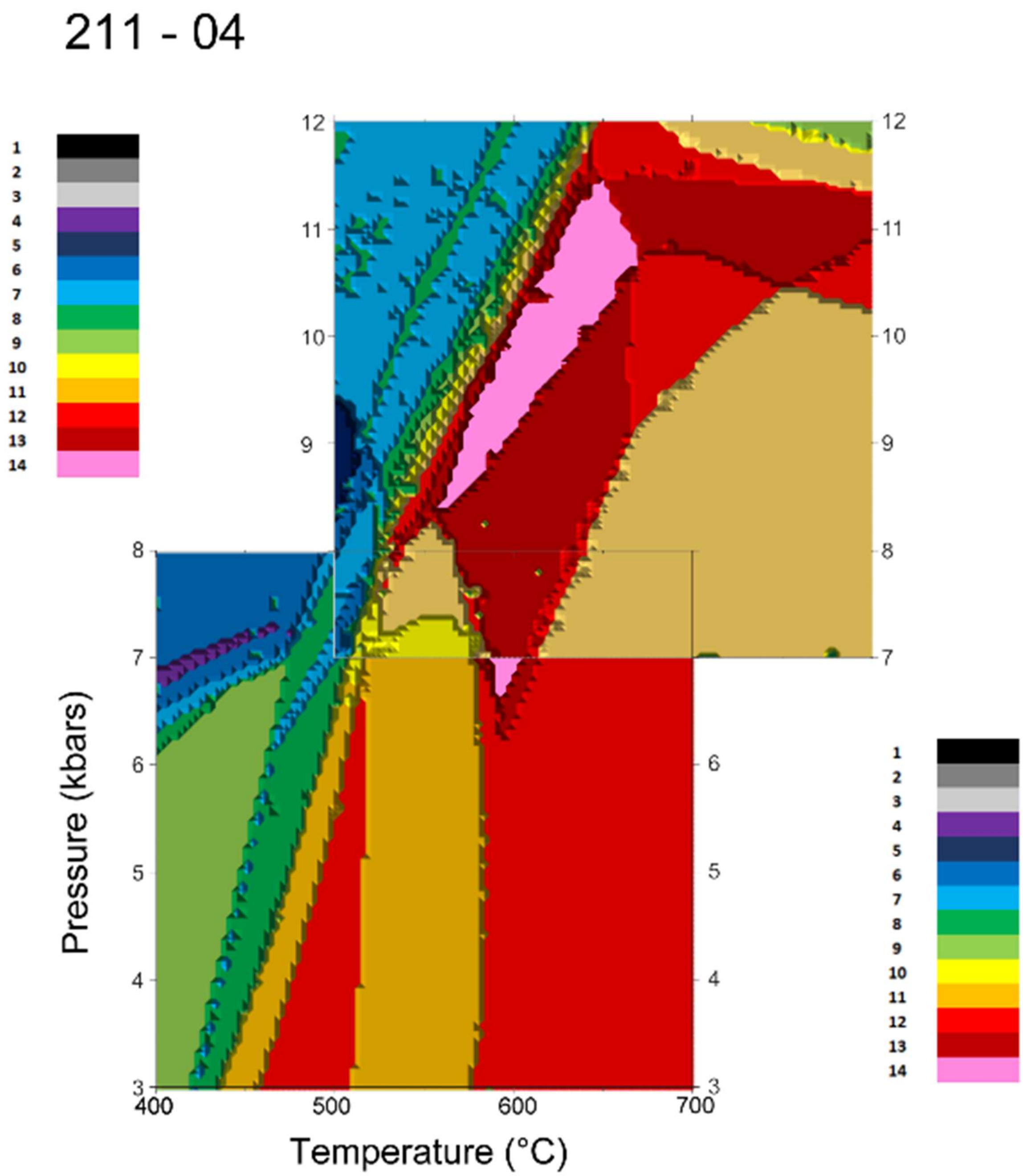

Figure 25. Perple_X thermodynamic model result for the coarse matrix assemblage of amphibolite sample 211. The minerals input into the assemblage include plagioclase, amphibole, and biotite. Pink represents the area with the most matching criteria in each section, whereas black has the fewest. There are 16 total criteria in both the low-pressure and high-pressure sections.

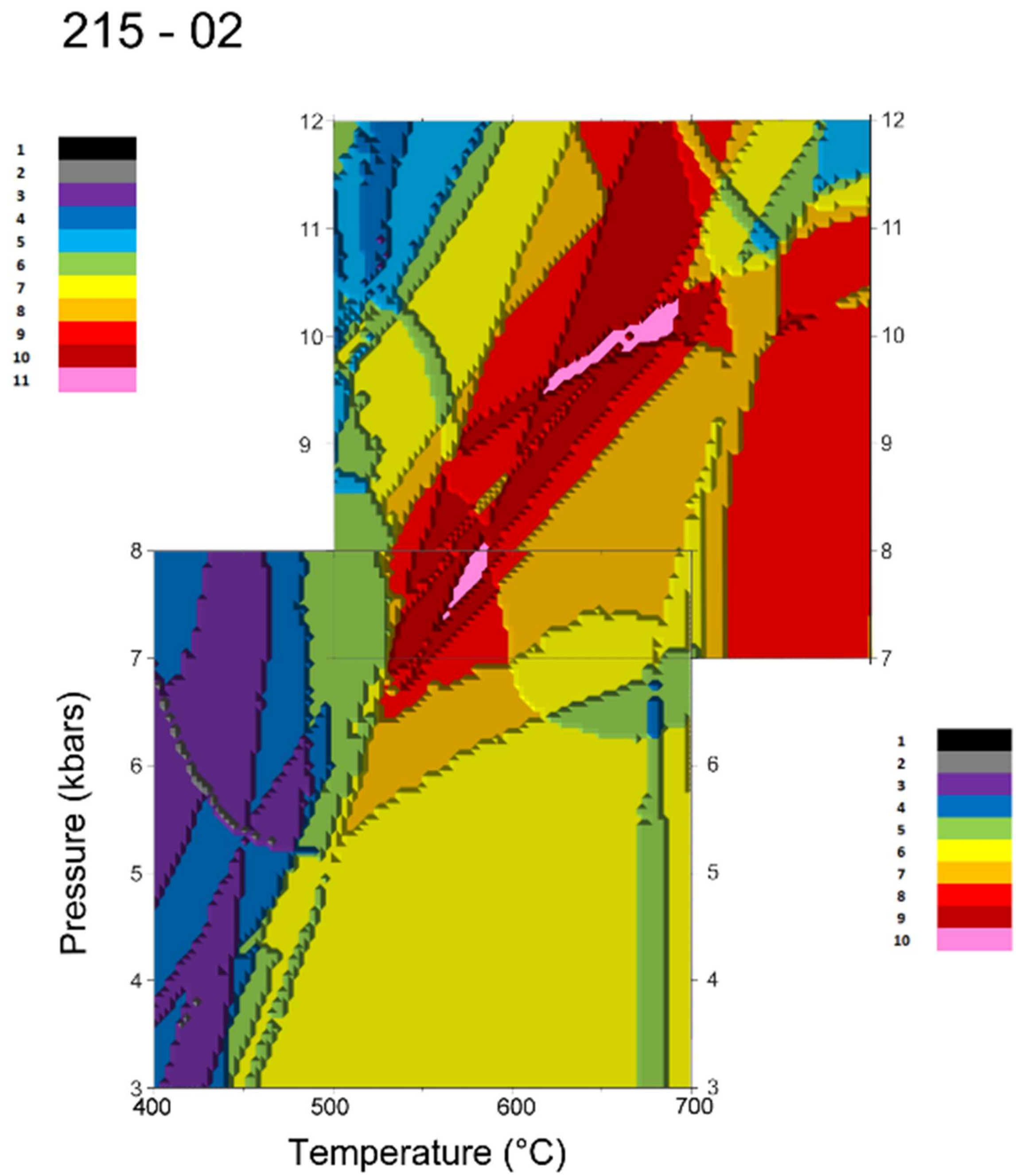

Figure 26. Perple_X thermodynamic model result for a recrystallized clinopyroxene symplectite in amphibolite sample 215. The minerals input into the assemblage include plagioclase, amphibole, and clinopyroxene. Pink represents the area with the most matching criteria in each section, whereas black has the fewest. There are 13 total criteria in the low-pressure section, and 14 in the high-pressure section.

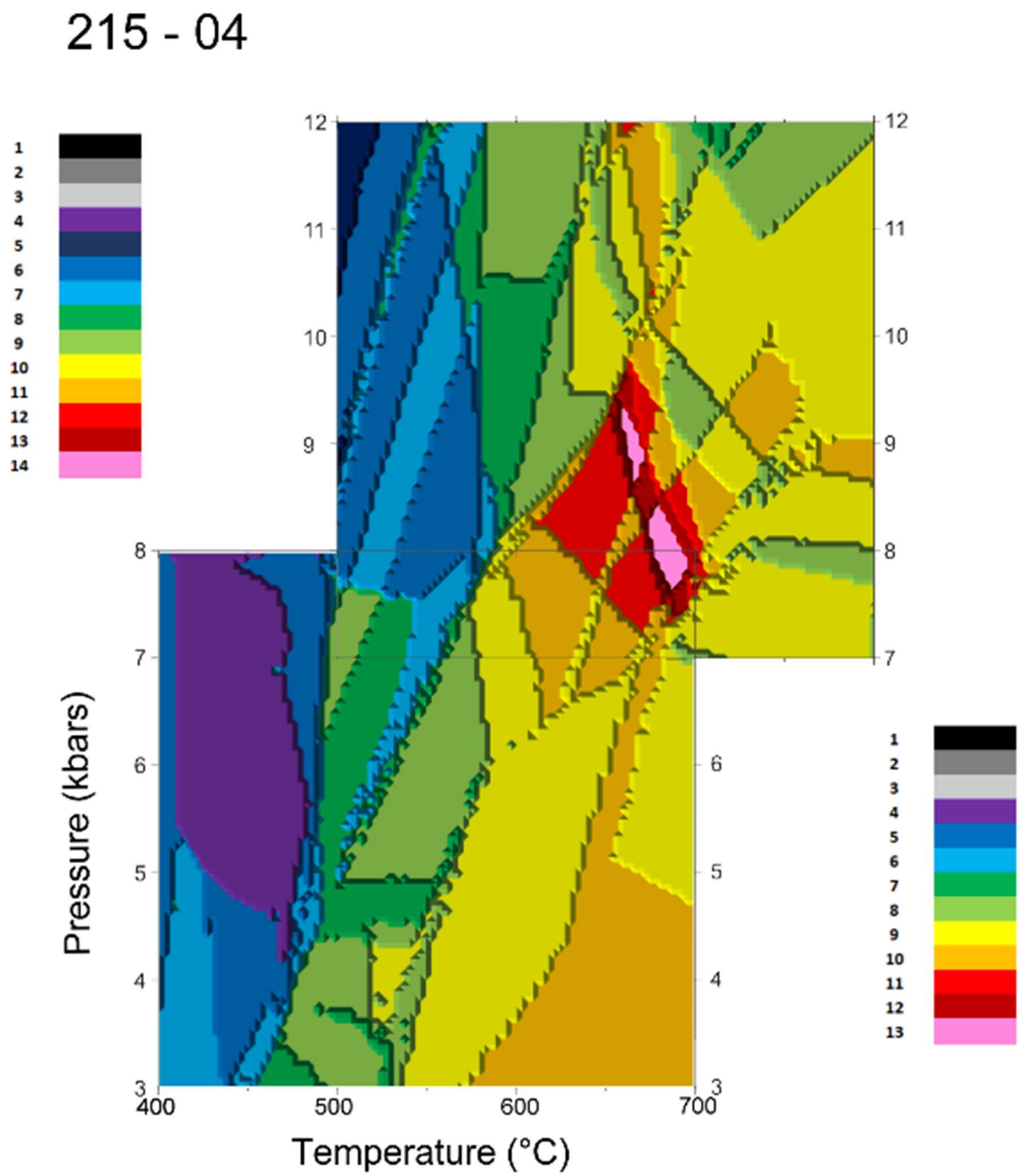

Figure 27. Perple_X thermodynamic model result for small hornblendes in a plagioclase moat surrounding garnet in amphibolite sample 215. The minerals input into the assemblage include plagioclase, amphibole, and garnet. Pink represents the area with the most matching criteria in each section, whereas black has the fewest. There are 16 total criteria in the low-pressure section, and 17 in the high-pressure section.

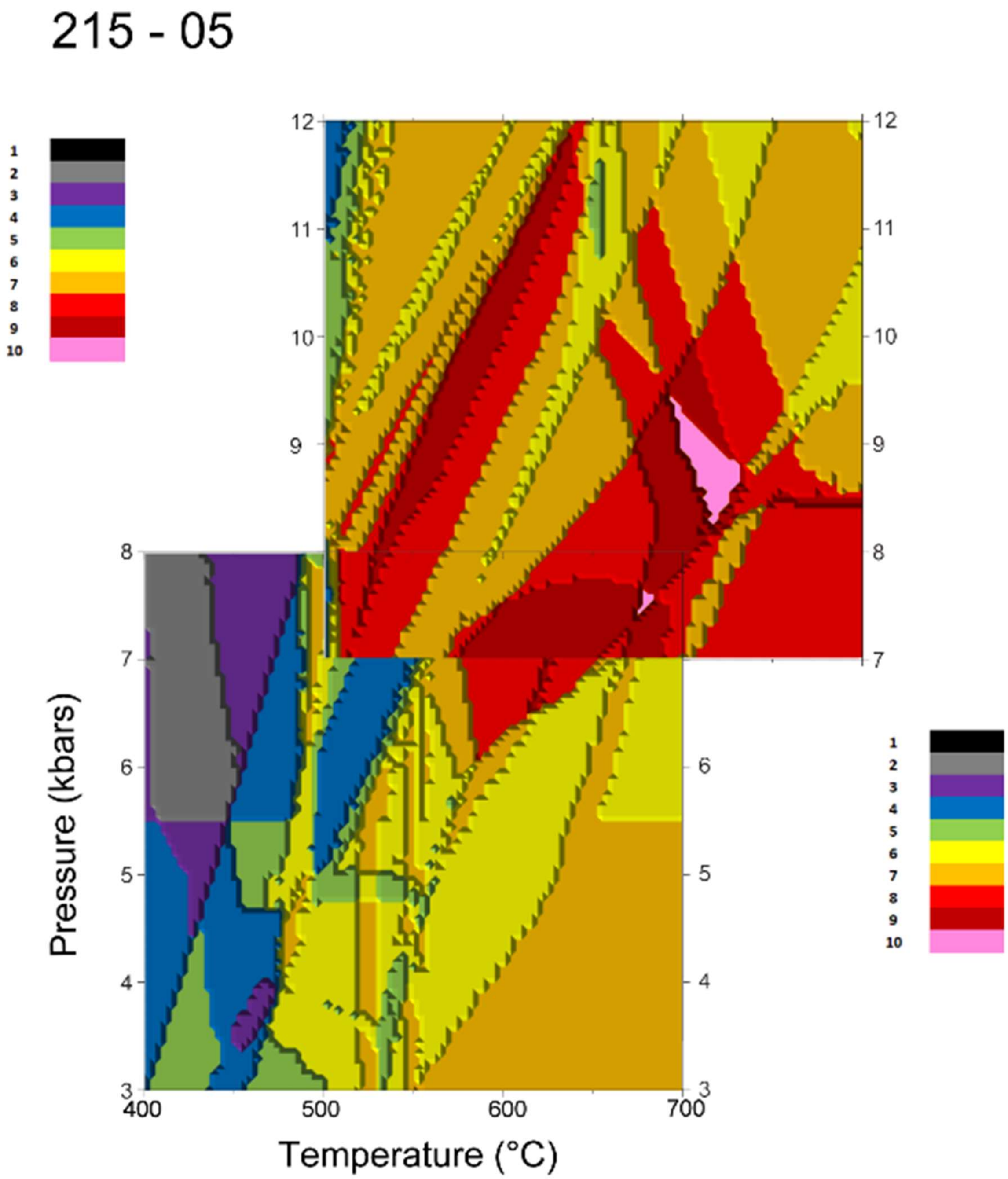

Figure 28. Perple_X thermodynamic model result for large hornblendes in a plagioclase moat surrounding garnet in amphibolite sample 215.The minerals input into the assemblage include plagioclase, amphibole, and garnet. Pink represents the area with the most matching criteria in each section, whereas black has the fewest. There are 14 total criteria in both the low-pressure and high-pressure sections.

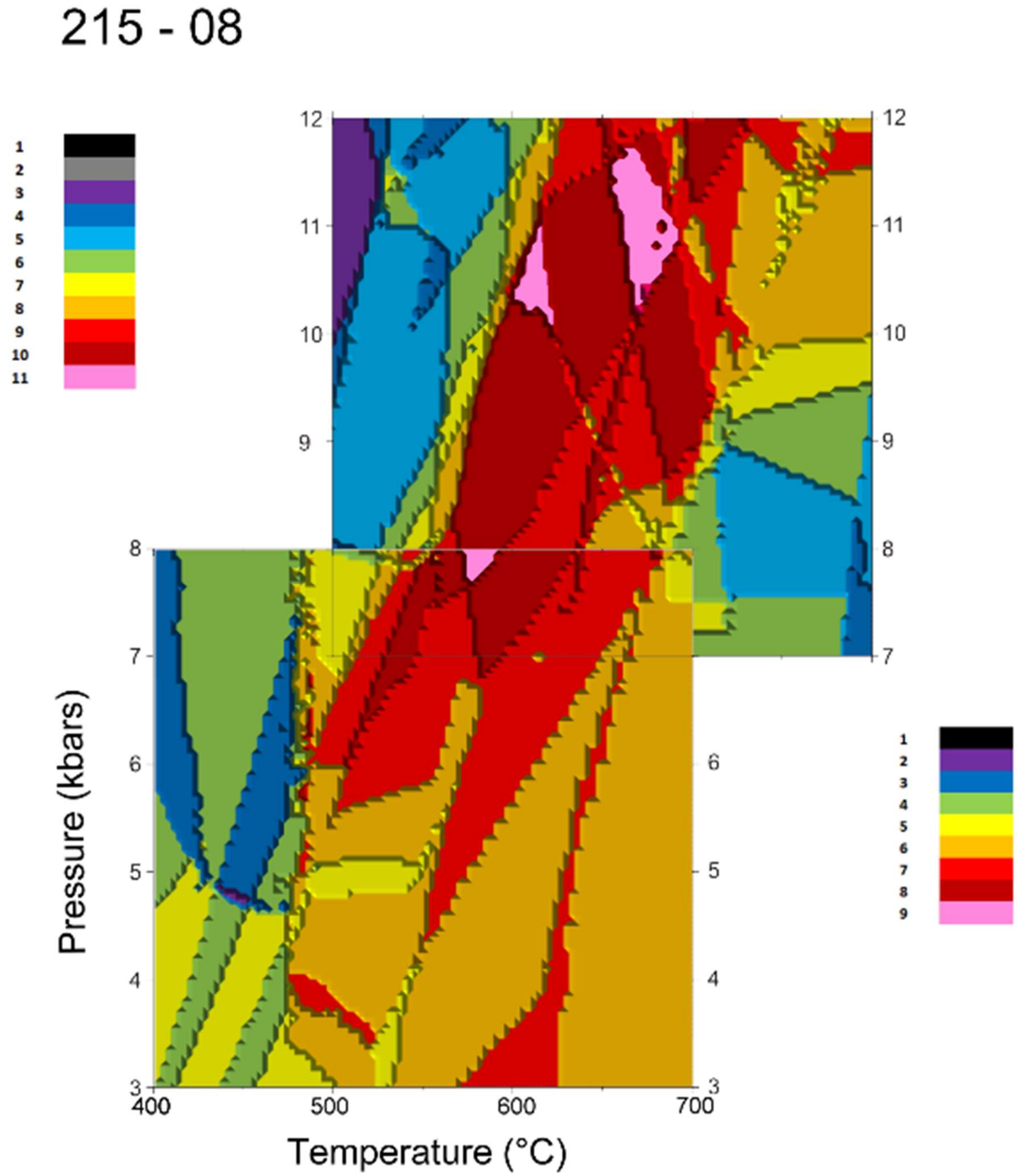

Figure 29. Perple_X thermodynamic model result for the matrix assemblage + garnet in amphibolite sample 215. The minerals input into the assemblage include plagioclase, amphibole, and garnet. There are 14 total criteria in both the low-pressure and high-pressure sections.

NOR-344

The fine-grained texture of 344 as well as the absence of garnet and presence f abundant, well-formed clinozoisite suggest that it is a fully recrystallized amphibolite. Consequently, NOR-344 thermodynamic models are taken to represent “end-product” eclogite re-equilibration into amphibolite facies conditions, rather than intermediate conditions found in remnant eclogite textures. From the wide range of mineral compositions, it was hard to determine which represented equilibrium assemblages, thus five main psuedosections were run, each with different combinations of clinozoisite, plagioclase, and amphibolite compositions. It was unclear if the system was saturated with quartz or not, but Perple_X thermodynamic modeling demonstrates that both saturated and unsaturated runs yielded similar T-P results, so either condition was viable. (Figures 30 and 31). These test runs, as well as two other models (Figures 32 and 33) all demonstrate a very consistent set of T-P conditions at ~500°C and 8 kbars. Models of 344-02s (Figure 32) and 344-04 (Figure 33) are presented as representatives of NOR-344 because they have the greatest number of matching criteria.

DISCUSSION

There was crude consistency of T-P results between the samples in the Blaho Nappe, but a comparison of T-P conditions is easier when all of the models are shown together. The Blåhø Nappe thermodynamic models were categorized as either symplectites or moat textures around garnets (representing post-eclogite retrograde conditions) or matrix (representing post-eclogite re-crystallized amphibolite) and were compiled into a single graph of T-P condition results (Figure 34). Eclogite temperature-pressure conditions were known to be in a T-P range of ~550–750°C and 15–35 kbars

(Carswell et al., 1985; Cuthbert et al., 2000; and Hacker 2007). Based on association with eclogite boudins and the abundant garnet symplectites and inclusion-rich diopsides, as well as garnet compositions, we concluded that the amphibolites of the Blåhø Nappe had once been eclogites themselves.

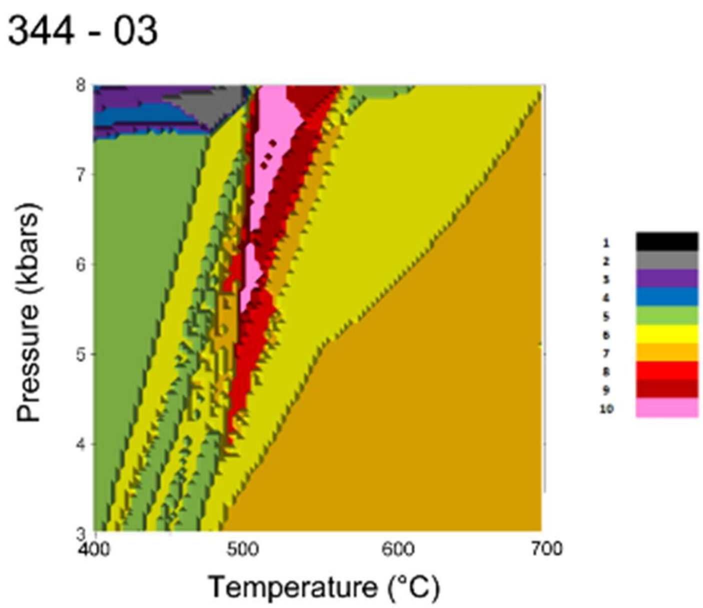

Figure 30. Perple_X thermodynamic model result for the matrix assemblage of amphibolite sample 344. The minerals input into the assemblage include plagioclase, amphibole, and epidote. There are 13 total criteria. This run was not quartz-saturated.

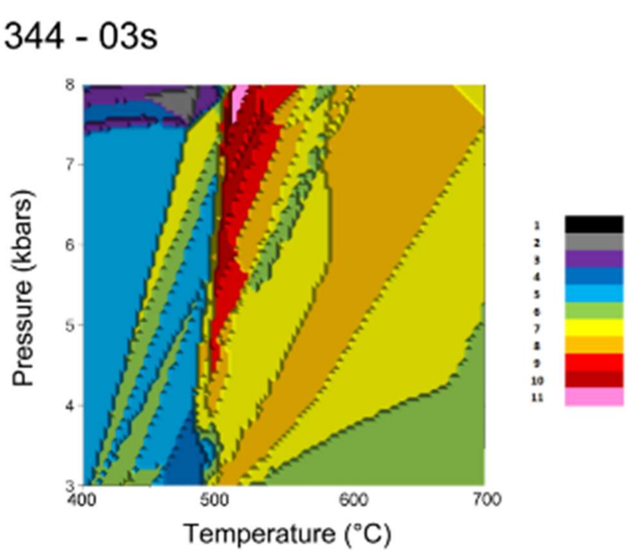

Figure 31. Perple_X thermodynamic model result for the matrix assemblage of amphibolite sample 344. The minerals input into the assemblage include plagioclase, amphibole, and epidote. There are 13 total criteria. This run was quartz saturated.

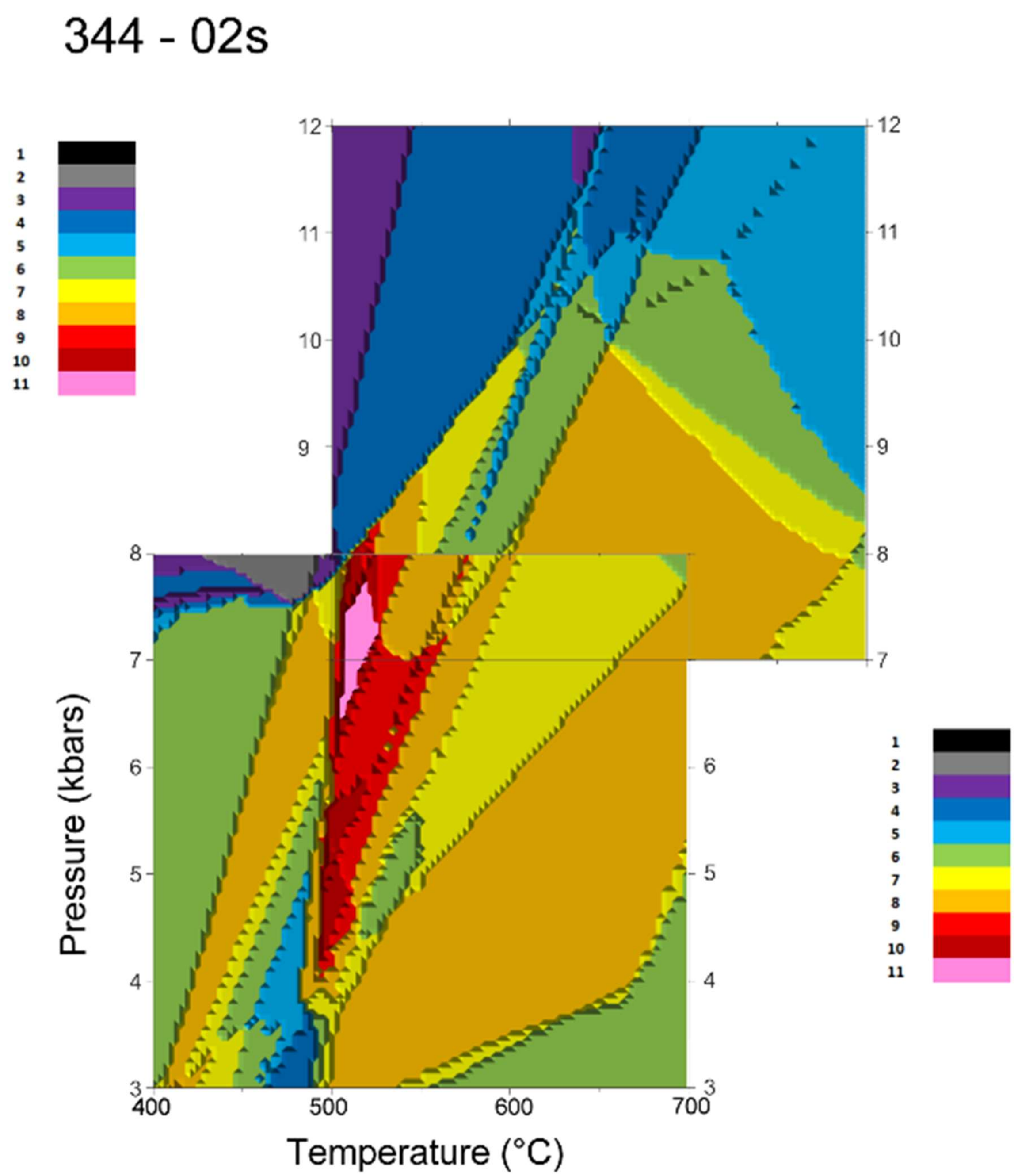

Figure 32. Perple_X thermodynamic model result for the quartz-saturated, matrix assemblage of amphibolite sample 344. The minerals input into the assemblage include high-An plagioclase, low-Al amphibole, and epidote. There are 13 total criteria in the low-pressure section, and 14 in the high-pressure section.

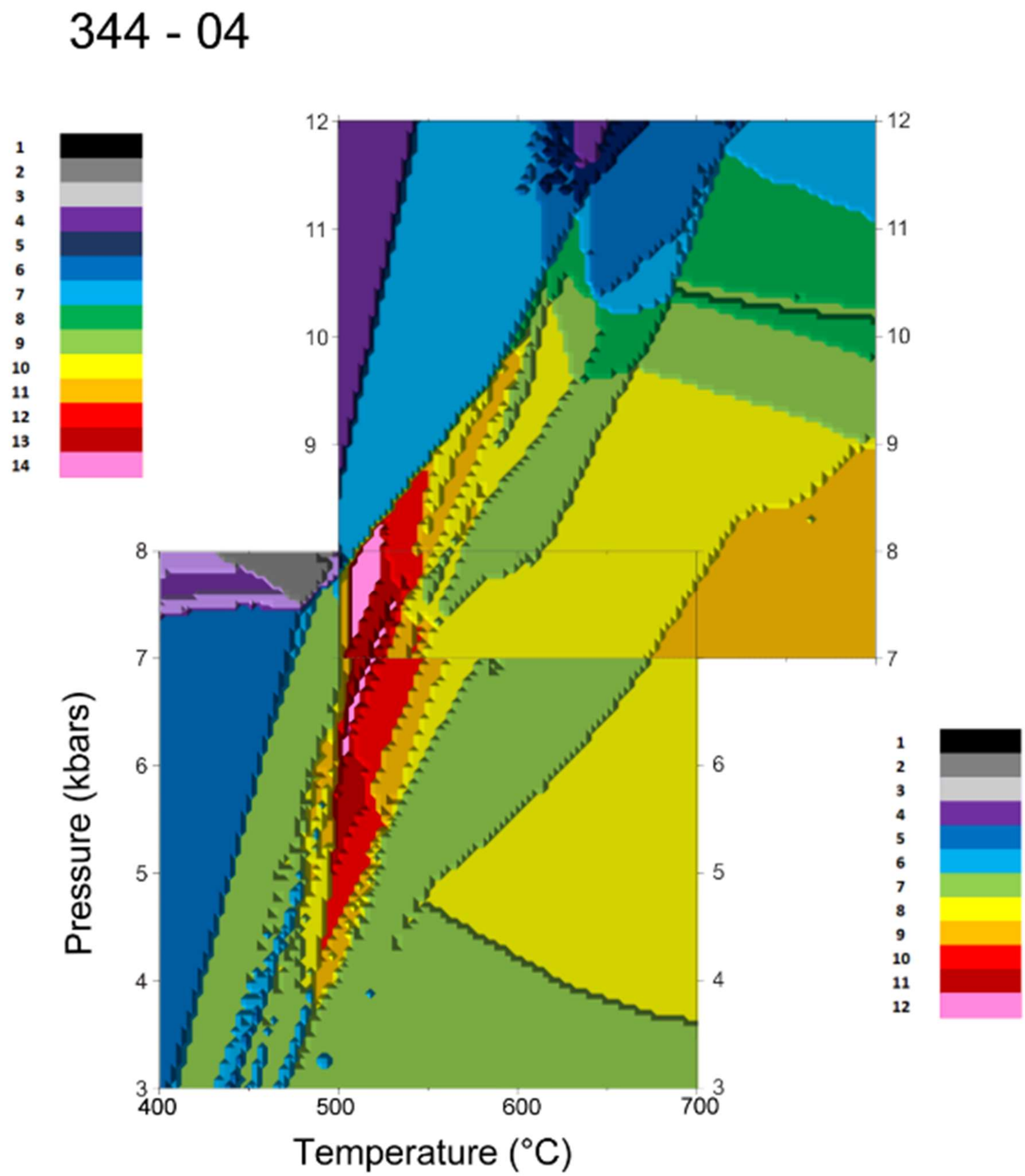

Figure 33. Perple_X thermodynamic model result for the matrix assemblage of amphibolite sample 344. The minerals input into the assemblage include high-An plagioclase, high-Al amphibole, and epidote. Pink represents the area with the most matching criteria, whereas black has the fewest. There are 13 total criteria in the low-pressure section, and 16 in the high-pressure section.

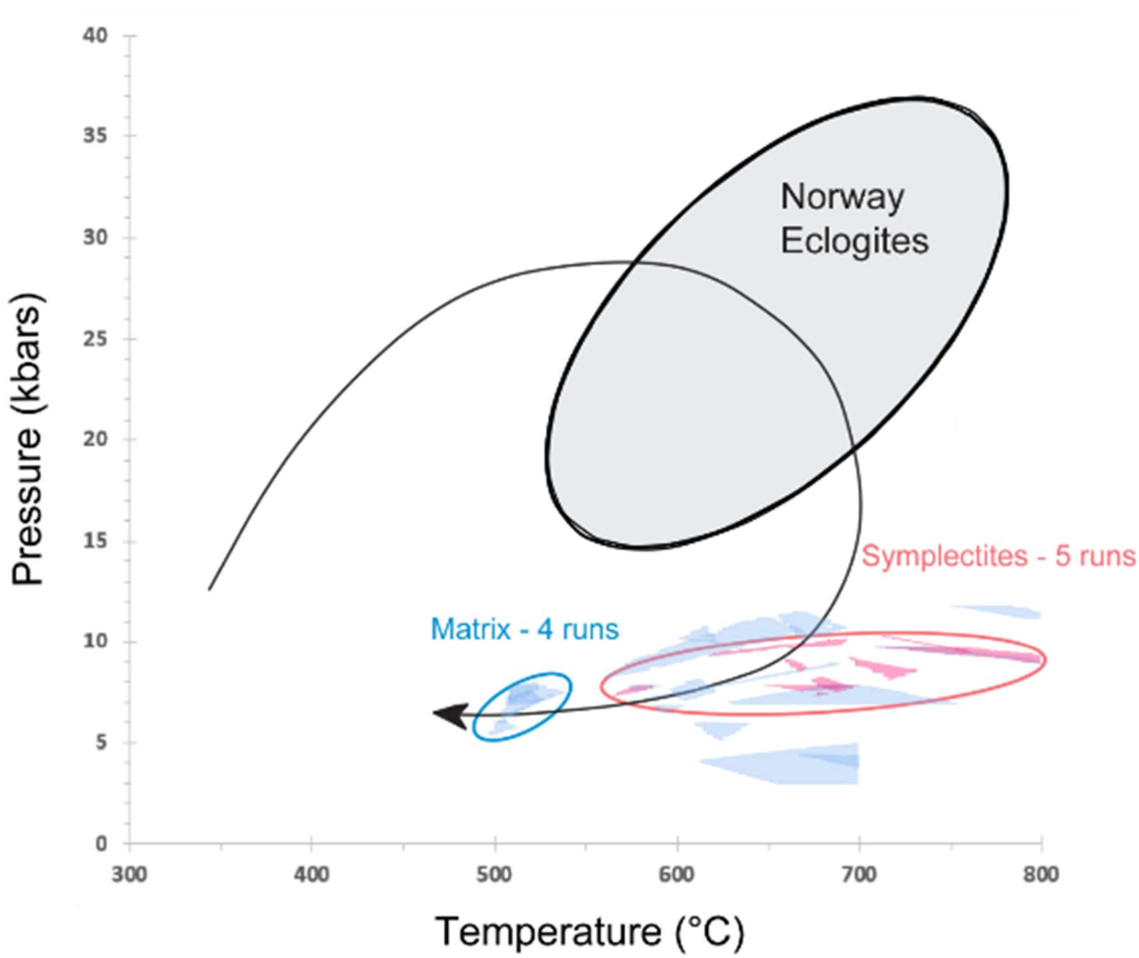

Figure 34. T-P path as Norway eclogites retrograded to Blåhø Nappe amphibolites, complied from thermodynamic modeling results. Symplectite (red fields) and matrix (blue fields) results are directly from the Perple_X thermodynamic models presented in this study, Figures 6 and 18-33, with the areas with most matching criteria shown colored. Symplectite refers to temperature-pressure conditions determined from remnant eclogite textures (primarily symplectites). Five symplectite runs were plotted, including data from samples NOR-191 (n=1), 204B (n=1), and 215 (n=3). All of these are included in the red ellipse. Matrix is coarse matrix from amphibolites, and implies the thoroughly recrystallized end-member T-P conditions of amphibolite re-equilibration. Matrix included 10 runs from a total of 6 samples: NOR-191 (n=1), 197A (n=2), 204B (n=1), 211 (n=2), 215 (n=1), and 344 (n=3) However, only four are included in the blue ellipse, which is inferred to be the most likely T-P conditions for amphibolite matrix re-crystallization. The blue ellipse include three runs from NOR-344, and one from NOR-215. The eclogite field (in gray circle) is based on Carswell et al.(1985), Cuthbert et al. (2000), and Hacker (2007).

The retrograded-eclogite domains (Figure 34, red fields) occur in a broad range of temperature conditions (550 - 800 °C) but a comparatively narrow range of pressures (7–10 kbars). This broad range of temperatures is due to the wide range of mineral compositions between samples, which may represent different degrees of disequilibrium. In any case, there was no justification for choosing any one of the symplectite T-P conditions over the others, thus this temperature range for remnant eclogite textures cannot be narrowed down in this study and it represents the best estimate of the T-P conditions for post-eclogite reequilibration (symplectites, etc.). However, despite the relatively wide range of temperature, the consistency of the pressures suggests that the determined pressure of 7–10 kbars maybe meaningful.

The matrix thermodynamic model results (Figure 34, blue fields) – representing re-equilibrated amphibolites – yielded wider scatter of T-P results. However, the scatter is interpreted to be a result of difficulty in determining which mineral compositions represented equilibrium conditions in different textural domains. In a single sample, ranges in hornblende composition and complex plagioclase zoning made it challenging to determine which set of compositions and textures were in equilibrium with each other at a given point in time. The scattered results probably indicate that most of those results are geologically meaningless, representing chosen mineral compositions that were never in equilibrium. The "best guess" for re-equilibrated amphibolite T-P conditions is at T-P conditions of ~475–525 °C, 5–8 kbars, where four runs match, including all the runs from NOR-344 as well as a run from NOR-215. None of the other matrix results were as consistent, neither internally nor when compared to different samples. NOR-344 was also the only sample without garnet, and was texturally the best example of a fully recrystallized amphibolite, making it an especially suitable representative for the "end-conditions" of the retrograding eclogites. The appropriateness of NOR-344 as a representative (due to mineral assemblage and texture) as well as the high consistency of Perple_X modeling results suggests that ~475–525 °C, 5–8 kbars were the conditions of the amphibolite matrix reequilibration.

CONCLUSIONS

Based on their association with eclogite blocks and having symplectite textures around garnet in many samples, amphibolites in the Blåhø Nappe were probably once Early Scandian eclogites themselves. These eclogites re-equilibrated into amphibolites along the approximated T-P path shown in Figure 34. Eclogites formed at temperatures of ~550–750°C and 15–35 kbars. Remnant eclogite textures in the Blåhø Nappe record T-P conditions of 550 - 800 °C, 7 - 10 kbars. Fully re-equilibrated amphibolite records metamorphic T-P conditions of ~475 - 525 °C, 5-8 kbars. Consistency within samples and between nearby samples is the only thing that indicates meaningful calculated temperatures and pressures of metamorphism, otherwise, because of the complexity of the mineral textures and chemistry, choosing apparent equilibrium textures was nearly impossible.

Future work should include thermodynamic modeling and additional geochemistry of more amphibolites as well as the felsic gneisses to better constrain this temperature-pressure path. More thermodynamic models of re-crystallized amphibolites may better constrain the end-result of eclogite re-equilibration in the Blåhø Nappe. Many of the felsic gneisses have the same minerals present as the amphibolites, though in very different proportions, but one sample contained kyanite, and may yield interesting results.

Additionally, recent software updates for the Perple_X thermodynamic modeling software, particularly bug-fixes for a newer pyroxene solution model (Augite(G), Green et al., 2016, as compared to Cpx(HP), Holland and Powell, 1996, with more recent updates). Bug fixes to the amphibole solution model, cAmph(DP) (Diener et al., 2011, with more recent updates) may also help.

REFERENCES

Brueckner, H. K., and Cuthbert, S. J., 2013, Extension, disruption, and translation of an orogenic wedge by exhumation of large ultrahigh-pressure terranes: Examples from the Norwegian Caledonides: Lithosphere, v. 5, p. 277–289.

Carswell, D.A., Krogh, E.J., Griffin, W.L., 1985, Norwegian orthopyroxene eclogites: calculated equilibration conditions and petrogenetic implications, *in* Gee, D.G., and Sturt, B.A. eds. The Caledonide Orogen - Scandinavia and Related Areas: Wiley, Chichester, p. 823–841.

Connolly, J.A.D. 2009, The geodynamic equation of state: What and how. : Geochemistry, Geophysics, Geosystems v. 10, p. 1–19. doi:10.1029/2009GC002540

Cuthbert, S. J., Carswell, D. A., Krogh-Ravna, E. J., and Wain, A. 2000, Eclogites and eclogites in the Western Gneiss region, Norwegian Caledonides: Lithos, v. 52, p. 165–195.

Eide, E. A., and Lardeaux, J. M., 2002, A relict blueschist in meta-ophiolite from the central Norwegian Caledonides—discovery and consequences: Lithos, v. 60, p. 1–19.

Gee, D. G., Fossen, H., Henriksen, N., and Higgins, A. K., 2008, From the early Paleozoic platforms of Baltica and Laurentia to the Caledonide Orogen of Scandinavia and Greenland: Episodes, v. 31, p. 44–51.

Green, E. C. R., White, R. W., Diener, J. F. A., Powell, R., Holland, T. J. B., and Palin, R. M., 2016, Activity–composition relations for the calculation of partial melting equilibria in metabasic rocks: Journal of Metamorphic Geology, v. 34, p. 845–869.

Hacker, B. (2007). Ascent of the ultrahigh-pressure Western Gneiss region, Norway: Geological Society of America Special Papers, v. 419, p. 171−184.

Hacker, B. R., and Gans, P. B., 2005, Continental collisions and the creation of ultrahigh-pressure terranes: Petrology and thermochronology of nappes in the central Scandinavian Caledonides: Geological Society of America Bulletin v. 117, p. 117–134.

Holland, T., and Blundy, J., 1994, Non-ideal interactions in calcic amphiboles and their bearing on amphibole–plagioclase thermometry: Contributions to Mineralogy and Petrology, v. 116, p. 433–447.

Hollocher, K., 1985, Geochemistry of metamorphosed volcanic rocks in the Middle Ordovician Partridge Formation, and amphibole dehydration reactions in the high-grade metamorphic zones of central Massachusetts. [Ph.D Thesis]: Department of Geology and Geography, Contribution #56, University of Massachusetts, Amherst, 275 p.

Hollocher, K., Robinson, P., Terry, M. P., and Walsh, E., 2007a, Application of major-and trace-element geochemistry to refine U-Pb zircon, and Sm/Nd or Lu/Hf sampling targets for geochronology of HP and UHP eclogites, Western Gneiss Region, Norway: American Mineralogist, v. 92, p. 1919–1924.

Hollocher, K., Robinson, P., Walsh, E., and Terry, M. P., 2007b, The Neoproterozoic Ottfjället dike swarm of the middle Allochthon, traced geochemically into the Scandian hinterland, Western Gneiss Region, Norway: American Journal of Science, v. 307 p. 901–953.

Hollocher, K., Robinson, P., Kennedy, C. and Walsh, E., 2015, Metamorphosed cumulate gabbros from the Støren Group of the Upper Allochthon, northern Western Gneiss Region, Norway: petrology and metamorphic record: Norwegian Journal of Geology, v. 94, p. 283–303.

Hollocher, K., Robinson, P., Seaman, K., and Walsh, E., 2016, Ordovician–early Silurian intrusive rocks in the northwest part of the Upper Allochthon, mid-Norway: Plutons of an Iapetan volcanic arc complex: American Journal of Science, v. 316, p. 925–980.

Krogh, E. J., 1980, Geochemistry and petrology of glaucophane-bearing eclogites and associated rocks from Sunnfjord, western Norway: Lithos, v.13, no. 4, p. 355–380.

Krogh, T.E., Kwok, Y., Robinson, P., and Terry, M., 2004, U-Pb constraints on the subduction-extension interval in the Averøya-Nordøyane area, Western Gneiss Region, Norway: Goldschmidt Conference, Abstract Volume, Copenhagen, Denmark, p. A101

Robinson, P. and Hollocher, K., 2008, Structural - metamorphic relationships between Caledonide nappes and Fennoscandian basement on the mainland near Brattvåg, in Robinson, P., Roberts, D., Gee, D.G. and Andréasson, P. G., eds, Guidebook: A tectonostratigraphic transect across the central Scandinavian Caledonides: International Geological Congress, 33rd annual meeting, Oslo, Norway, Part II, Day 8, p. 1−16.

Terry, M. P., Robinson, P., and Ravna, E. J. K., 2000, Kyanite eclogite thermobarometry and evidence for thrusting of UHP over HP metamorphic rocks, Nordøyane, Western Gneiss Region, Norway: American Mineralogist, v. 85 p. 1637-1650.

Terry, M. P., and Robinson, P., 2003, Evolution of amphibolite-facies structural features and boundary conditions for deformation during exhumation of high-and ultrahigh-pressure rocks, Nordøyane, Western Gneiss Region, Norway: Tectonics, v. 22, p. 1–23, 1036, doi:10.1029/2001TC001349.

Tucker, R.D., Robinson, P., Solli, A., Gee, D.G., Thorsnes, T., Krogh, T.E., Nordgulen, Ø. A, and Bickford, M.E., 2004, Thrusting and extension in the Scandian hinterland, Norway: New U–Pb ages and tectonostratigraphic evidence: American Journal of Science v. 304, p. 477–532.

Winter, J.D., 2010, Principles of Igneous and Metamorphic Petrology, Second Edition: Upper Saddle River, New Jersey, Pearson Prentice Hall, 579 – 606 p.

APPENDIX 1

Table 1. Description of mineral phases present in 23 samples examined in thin section (felsic gneisses and amphibolites)

Sample #	Mineral phases present								
	Garnet	Hornblende	Biotite	Quartz	Plagioclase	Epidote	Clinopyroxene	Titanite	Rock Type
NOR-112		Y	Y	Y	Y	Y		Y	Amphibolite
NOR-129	Y	Y	Y	Y	Y	Y		Y	Amphibolite
NOR-153		Y	Y		Y	Y		Y	Amphibolite
NOR-156*	Y	Y	Y	Y	Y				Felsic Gneiss
NOR-173	Y	Y	Y	Y	Y				Amphibolite
NOR-191*	Y	Y			Y	Y	Y		Amphibolite
NOR-197A*	Y	Y		Y	Y	Y	Y	Y	Amphibolite
NOR-197B	Y	Y		Y	Y		Y	Y	Amphibolite
NOR-199	Y	Y	Y	Y	Y		Y		Amphibolite
NOR-201	Y	Y	Y	Y	Y				Amphibolite
NOR-203	Y	Y	Y	Y	Y	Y	y	Y	Felsic Gneiss
NOR-204B*	Y	Y			Y		Y		Amphibolite
NOR-210	Y	Y	Y		Y	Y	Y		Amphibolite
NOR-211*	Y	Y	Y		Y			Y	Amphibolite
NOR-212	Y	Y	Y		Y				Amphibolite
NOR-215*	Y	Y	Y	Y	Y		Y		Amphibolite
NOR-237	Y	Y	Y	Y	Y	Y			Amphibolite
NOR-315	Y	Y	Y	Y	Y	Y		Y	Amphibolite
NOR-325		Y	Y	Y	Y	Y	Y	Y	Amphibolite
NOR-344*		Y	Y	Y	Y	Y	Y	Y	Amphibolite
NOR-358*		Y			Y	Y		Y	Amphibolite
NOR-362	Y	Y		Y	Y	Y		Y	Amphibolite
NOR-367	Y	Y		Y	Y	Y	Y	Y	Amphibolite

Note: Sample numbers marked with an asterisk (*) were used for Perple_X runs.

APPENDIX 2

Table 4. Model rock compositions used in Perple_X. Includes 1 felsic gneiss (NOR-156), and 6 amphibolites (NOR 197A – 344).

Sample	Run	Model rock composition (weight %)										Minerals Included	Purpose
		Na_2O	MgO	Al_2O_3	SiO_2	K_2O	CaO	TiO_2	FeO	Fe_2O_3	H_2O		
156	1	2.98	2.84	21.92		3.39	4.15	0.01	17.89	1.08	5	Plag, Gar, Bio	Matrix
	2	2.87	3.1	20.33		2.59	5.94	0.01	19.06	1.62	5	Hbl, Plag, Gar, Bio	Matrix
197A	1	2.16	6.26	16.25			14.58	0.01	12.06	0.37	5	Hbl, Plag, Cpx	Matrix
	2	1.56	6.42	15.98			15.33	0.01	12.31	0.47	5	Hbl, Plag, Cpx	Matrix
	3	2.49	4.47	20.24			11.88	0.01	13.11	0.59	5	Hbl, Plag	Matrix
	4	3.36	7.84	14.21			14.32	0.01	7.4	0.37	5	Hbl, Plag, Cpx	Matrix
	5	2.87	7.92	13.88			15.17	0.01	7.67	0.44	5	Hbl, Plag, Cpx	Matrix
191	1	3.59	8.98	12.32	53.52		14.23	0.01	5.93	1.43	5	Hbl, Plag, Cpx	Symplectite
	2	4.25	8.35	12.88	52.72		13.32	0.01	5.74	1.74	5	Hbl, Plag, Cpx	Matrix
	3	3.49		27.4	48.8		16.36	0.01		3.95	5	Epi, Plag	High Pressure
	4	4.02	8.85	14.04	52.49		13.82	0.01	5.83	0.96	5	Hbl, Plag, Cpx	Matrix
	5	4.37	8.27	15.24	52.04		13.17	0.01	5.4	1.49	5	Hbl, Plag, Cpx	Matrix
	6	2.95	5.4	21.73	45.56		10.67	0.01	11.94	1.75	5	Hbl, Plag, Gar	Symplectite
	7	4.84	5.35	19.96	50.79		9.99	0.01	6.38	2.68	5	Hbl, Plag	Symplectite
	8	4.93	5.71	14.85	56.05		13.56	0.01	3.15	1.75	5	Plag, Cpx	Symplectite
	9	2.82	6.94	17.03	47.63		12.91	0.01	10.46	2.21	5	Hbl, Plag, Cpx, Gar	Symplectite
	10	3.03	5.48	21.9	45.59		10.65	0.01	12.13	1.23	5	Hbl, Plag, Gar	Symplectite
204B	1	1.63	7.02	23.94	43.38		12.91	0.01	9.94	1.18	5	Hbl, Plag, Gar	Symplectite
	2	5.02	6.97	20.36	51.5		10.18	0.01	5.02	0.96	5	Hbl, Plag	Matrix
	3	5.04	6.79	20.88	51.08		10.11	0.01	4.82	1.29	5	Hbl, Plag	Matrix
	4	1.53	7.19	24.08	43.28		12.94	0.01	9.5	1.48	5	Hbl, Plag, Gar	Symplectite
	5	3.26	8.81	15.93	50.96		14.55	0.01	4.82	1.33	5	Hbl, Plag, Cpx	Symplectite
	6	2.52	9.06	17.31	48.68		16.04	0.01	4.49	1.56	5	Hbl, Plag, Cpx	Matrix
	7	2.31	9.04	16.75	48.98		15.89	0.01	4.52	2.18	5	Hbl, Plag, Cpx	Matrix
211	1	3.76	6.37	20.69	47.97		9.34	0.01	11.36	0.5	5	Hbl, Plag, Gar	Symplectite
	2	3.87	6.16	20.98	46.98		9.03	0.01	11.48	0.49	5	Hbl, Plag, Gar	Symplectite
	3	3.86	6.09	21.47	47.73		8.93	0.01	11.16	0.76	5	Hbl, Plag, Gar	Symplectite
	4	4.02	9.32	20.02	48.76	3.54	5.52	0.01	8.3	0.52	5	Hbl, Plag, Bio	Matrix
215	1	4.43	8.77	12.65			12.97	0.01	6.3	1.02	5	Hbl, Plag, Cpx	Matrix
	2	3.95	8.01	15.37			13.37	0.01	6.76	1.09	5	Hbl, Plag, Cpx	Symplectite
	3	4.6	6.37	14.46			13.86	0.01	3.52	0.81	5	Plag, Cpx	Symplectite
	4	1.92	6.28	23.39			12.39	0.01	11.31	0.83	5	Hbl, Plag, Gar	Symplectite
	5	2.82	6.21	22.47			11.11	0.01	11.43	0.71	5	Hbl, Plag, Gar	Symplectite
	6	4.15	2.85	23.27			8.02	0.01	11.72		5	Plag, Gar	Garnet Interior
	7	5.81	6.41	18.9			8.85	0.01	5.92	1.02	5	Hbl, Plag	Matrix
	8	3.87	6.42	19.95			9.13	0.01	11.54	0.68	5	Hbl, Plag, Gar	Matrix
344	1	3.93	3.84	22.14	50.08		13.41	0.01	4.28	2.32	5	Epi, Plag, Hbl	Matrix
	1s	3.93	3.84	22.14			13.41	0.01	4.28	2.32	5	Epi, Plag, Hbl	Matrix
	2	3.74	3.84	22.41	49.67		13.43	0.01	4.28	2.32	5	Epi, Plag, Hbl	Matrix
	2s	3.74	3.84	22.41			13.43	0.01	4.28	2.32	5	Epi, Plag, Hbl	Matrix
	3	4.01	3.67	22.46	49.84		13.32	0.01	4.33	2.36	5	Epi, Plag, Hbl	Matrix
	3s	4.01	3.67	22.46			13.32	0.01	4.33	2.36	5	Epi, Plag, Hbl	Matrix
	4	3.83	3.67	22.74	49.43		13.64	0.01	4.33	2.36	5	Epi, Plag, Hbl	Matrix
	4s	3.83	3.67	22.74			13.64	0.01	4.33	2.36	5	Epi, Plag, Hbl	Matrix
	5	4.59	3.57	20.91	50.68		12.31	0.01	4.46	3.48	5	Epi, Plag, Hbl	Matrix
	5s	4.59	3.57	20.91			12.31	0.01	4.46	3.48	5	Epi, Plag, Hbl	Matrix

Note: K_2O was only included in model rocks containing biotite. SiO_2 was excluded from the model rock compositions if the system was set to be silica-saturated (i.e. quartz was always present in the model). Mineral abbreviations: Plag = plagioclase, Gar = garnet, Bio = biotite, Hbl = hornblende, Cpx = clinopyroxene, and Epi = epidote.